# Deciduous Tooth Resorption after Overfilling of Root Canal Filler: Function and Nature of Multinucleated Giant Cells

Hiromasa Hasegawa
Motoyoshi Antoh
Noriyuyki Takei
Takanaga Ochiai

《**Abstract**》

There are numerous reports on physiological root resorption claiming that the root resorption process of primary teeth is regulated in a manner similar to bone remodeling [28]. However, complex histological changes occur under several pathological conditions. Abnormal tooth resorption could be found in primary teeth due to certain causes until the completion of the permanent dentition. In Japan and eastern Asia, calcium hydroxide paste with silicon oil added iodoform is widely used for endodontic treatment of deciduous teeth. This material is sometimes excessively filled within root canals, and pathological reactions have been already discussed in previous sections. In this part, the influences on deciduous tooth endodontic therapy will be described in detail. The most characteristic feature is abnormal tooth resorption via osteoclast-like multinucleated giant cells (MGCs) and foreign body giant cells (FBGCs). In the later part of this section, the characteristics of foreign body type giant cells will be discussed through *in vivo* experiments.

## Influence of Excess Root Canal Filler upon Deciduous Teeth

To examine the influence of inadequate root canal filling, the following experiment was planned. The second and third deciduous lower molars received pulpectomy, root canal preparation, and root canal filling using Vitapex® composed of 30.3% of calcium hydroxide, 40. 4% of iodoform and 22.4% of silicone oil, under general anesthesia. Contralateral molars without treatment served as controls. Roentgenographic examinations were performed after filling, 2, 4 and 8 weeks after treatments. The following data are for the experiments in dogs from 2 to 3. 5

months of age. Root surfaces of deciduous teeth showed that numerous MGCs seem to be derived by stimuli based on excessive filling paste which flowed out from the apical foramen, showing that root resorption of experimental teeth might be earlier than that of controls.

### 1) Acceleration of deciduous tooth resorption via excess filler

Roentgenograms showed that the second and the third deciduous lower molars were incompletely formed. At this stage, permanent teeth crowns were of low radiopaque appearance without root formation (Figure 1, a, b, e and f). Controls without treatment showed no root resorption 4 weeks and 8 weeks after operation (Figure 1, c and g). Compared with these controls, examples with adequate root filling also demonstrated no significant changes after eight weeks (Figure 1, h). As mentioned above, this experiment was designed to study experimental teeth which received root canal preparation and root filling between 2 to 3. 5 months after birth. This stage is consistent with findings from the late root formation stage to the root stable stage of deciduous dentitions, in which root apices were almost closed. Roots which were adequately filled showed the same findings as those of controls. Root apices appeared to be stable and permanent teeth were successfully developing 8 weeks after filling (Figure 1, h).

Radiographic changes of deciduous teeth with overfilling are of interest, since intentionally overfilled paste flows out around the permanent tooth germs. The amounts of overflowed paste are variable by case. In some cases, a large amount of the paste covers a tooth crown (Figure 1, b). Two weeks after the operation, the radiopacity of the excess paste decreased without obvious root resorption of deciduous teeth. Four weeks after the operation, the radiopacity of the excess filling paste declined significantly, and for ones measuring about a few millimeters in diameter, it completely disappeared. However, a large amount of the paste flowed into periapical tissue and around permanent tooth crowns, where it seemed to be hardly absorbed (Figure 1, d). In this stage, roughly half of excessively filled cases showed root resorption, accompanied by remarkable examples showing more than half-length resorption. Eight weeks after root canal filling, the trabecular-radiopaque feature was observed in the area where the excess paste was absorbed. The resorption was also detected in roots with excessively filled paste, but there were no distinctive root resorption in adequately treated cases (Figure 1, h).

Light microscopic observations confirmed some evidence of radiographic changes. In controls and adequately filled cases, there were no significant histological changes 2 or 4 weeks after experimental start. The paste was filled neither over nor under in root canals, accompanied by no inflammatory cells in the apical periodontal tissue. Root apices were completely formed without physiological root resorption (Figure 2, a). In 8-week cases, some kinds of deciduous teeth reached the exchanging stage. Once physiological root resorption occurred, the filling paste appeared in the periodontal tissue along with the progression of root resorption. The filling material was surrounded by inflammatory cell-rich granulation tissue with some vacuoles. New trabecular bone also formed with the absorbing paste (Figure 2, b). Excess paste widely flowed not only into the periapical tissue, but also into spaces between the permanent teeth and bone, and sometimes the paste directly touched permanent tooh germs. Two weeks after the treatment, root resorption was infrequent and slight (Figure 2, c). The granulation tissue surrounding the paste comprised numerous foamy cells, large irregular cells having ovoid nucleus, spindles cells, and MGCs (Figure 2, d).

In 4-week examples, excessively filled cases showed marked root resorption compared with controls and adequately treated cases. The extruded paste scattered throughout the periodontal tissue and surrounded by the granulation tissue contained the same kinds of cells as
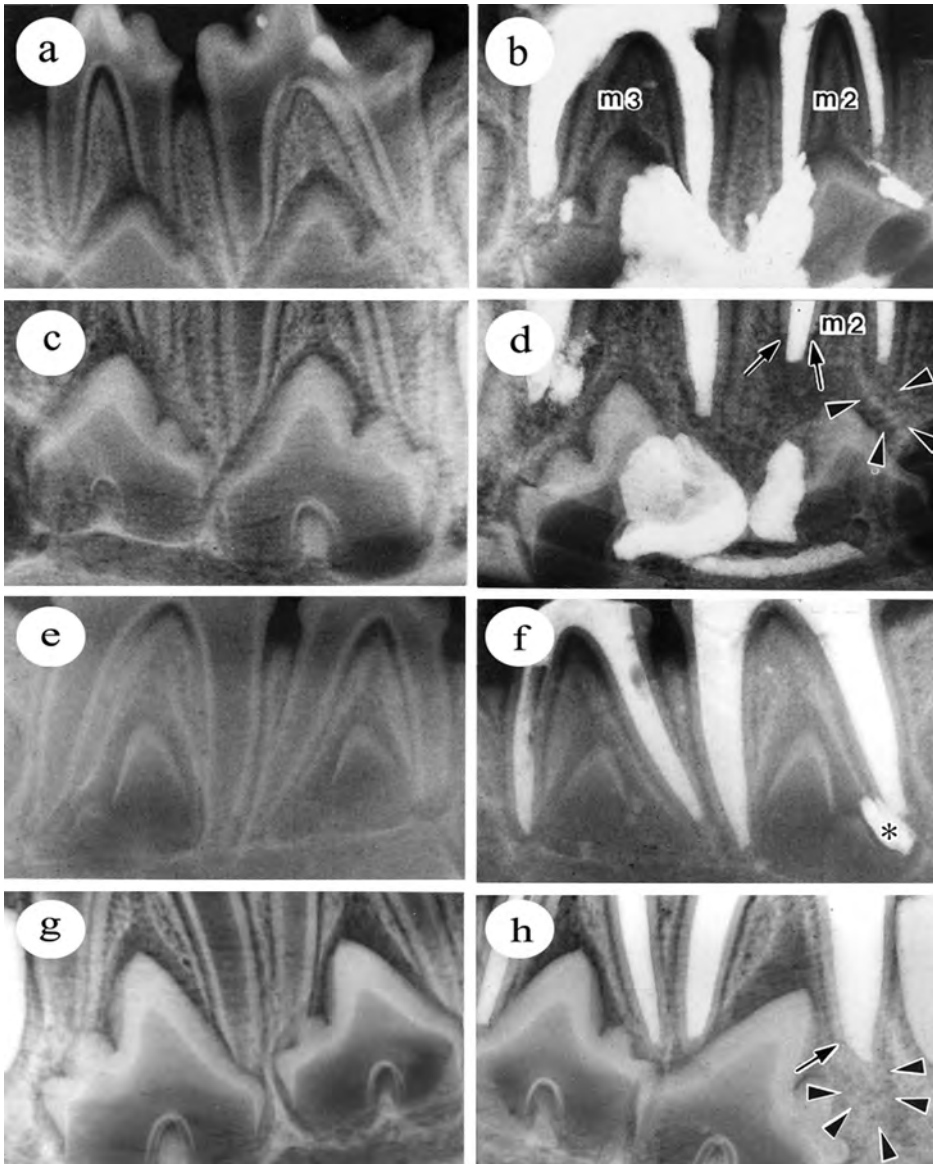
**Figure 1**    Radiographic feature sets of a 4-week (a-d) and 8-week group (e-h)

a: Root apices are incompletely formed at the beginning of the experiment. Permanent teeth also show incompletely formed crowns with poor radiopacity.

b: This case shows variable amounts of the overfilled paste just after the treatment.

c: Four weeks after the start of experiment, the control displays shows no significant root resorption and normal progression of permanent teeth.

d: Radiopaque features of the excess paste decrease, especially a small amount of the extruded paste is completely absent (arrow heads). Note abnormal root resorption (arrows).

e: The feature of the beginning is same as that of Figure 1, a.

f: In this case, only a small amount of the excess paste (asterisk) is observed.

g: After 8 weeks, a control specimen shows normal development of permanent teeth.

h: Eight weeks after the operation, a small amount of excess paste is completely absorbed with the feature of trabecular radiopacity (arrow heads). The root close to the excess paste is absorbed (arrow).
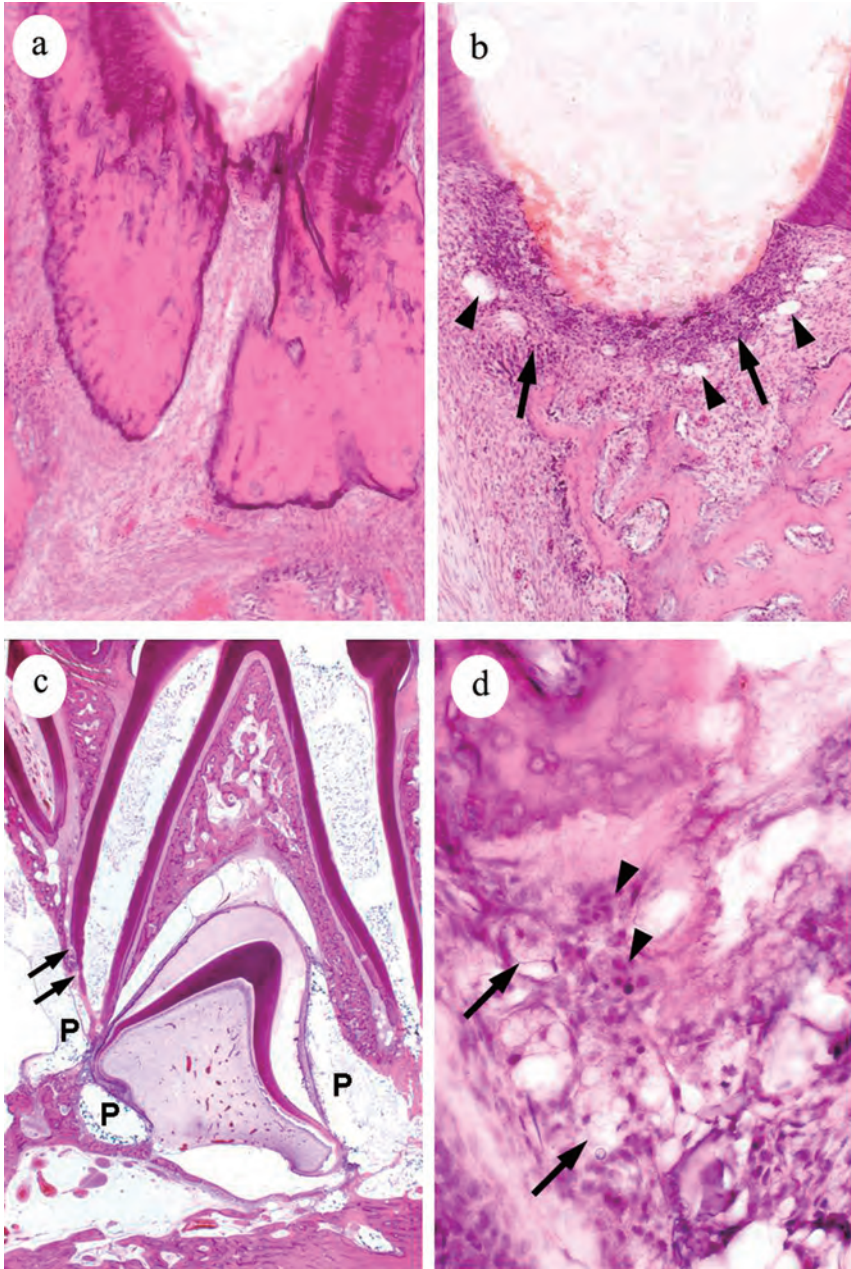
**Figure 2**    Histological features after root canal filling
a:  An adequately filled case shows no inflammatory changes in the apical periodontal
    tissue 2 weeks after the operation.
b:  Eight weeks after operation, the filling paste is covered by marked inflammatory cell
    infiltration (arrows) as physiological root resorption even in an adequate case. Some
    vacuoles appear in the granulation.
c:  A large amount of the excess paste is observed as cavities (P) with slight root
    resorption (arrows) 2 weeks after the root filling.
d:  A two-week example shows multinucleated giant cells (arrow heads) and foamy cells
    (arrows) infiltrating around the excess paste.
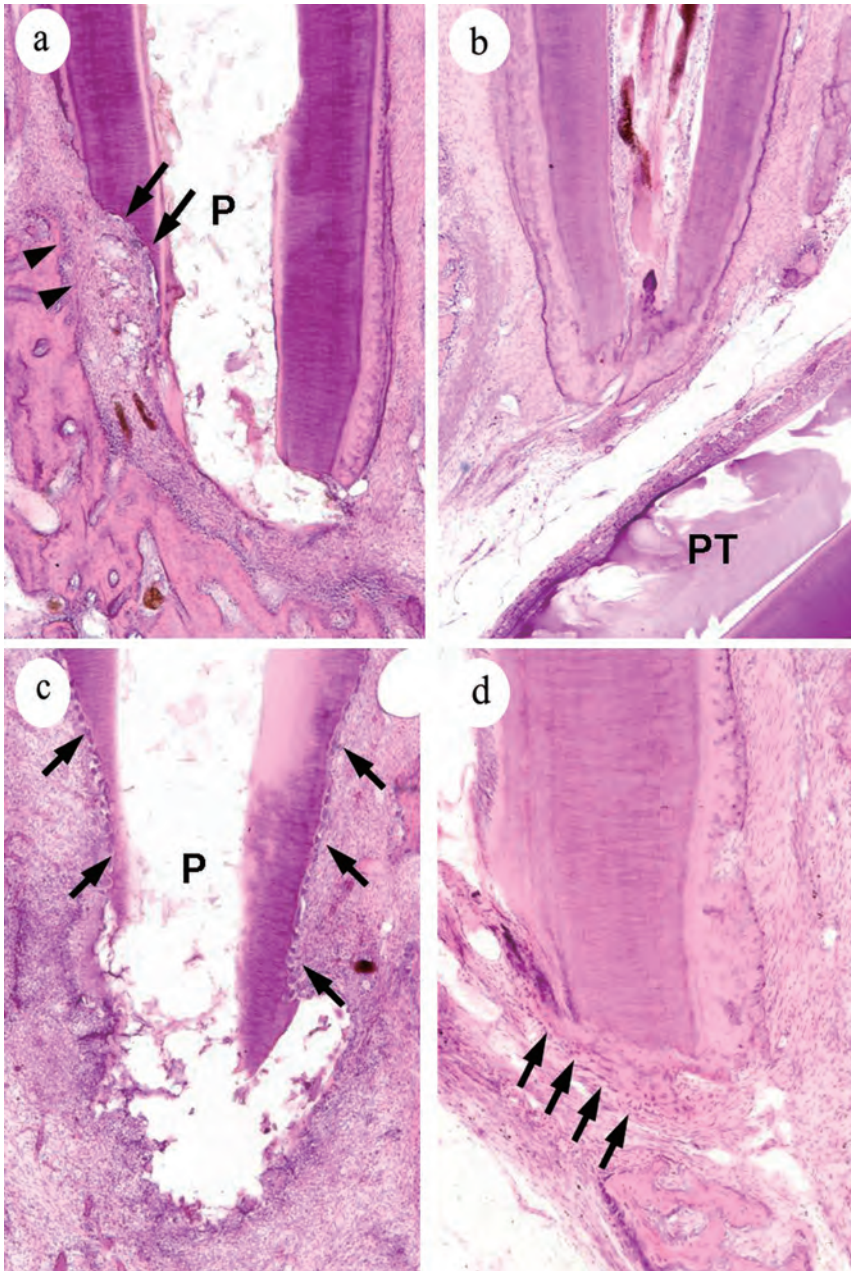
**Figure 3**    Histological changes 4 weeks after the treatment

a:  Excess paste (asterisk) distributes through the periodontal tissue with the marked resorption cavity formation and bone formation (arrow heads). Note no resorption on the root surface of the opposite side. P: filling paste

b:  The contra-lateral tissue of Figure 3, a shows no significant changes with a completely formed root apex and a normal looking permanent tooth (PT)

c:  An instance of significant root resorption shows that numerous odontoclasts align on the dentin surface (arrows).

d:  The contra-lateral side of Figure 3, c shows that the root apex with mild resorption is recovered by cementum deposition (arrows).

the 2-week samples. Resorption lacunae frequently formed in front of the granulation tissue treated with excess paste (Figure 3, a), but the contra-lateral, control roots were stable without resorption (Fiure 3, b). In significant instances, more than half of the deciduous root in length was removed by numerous odontoclasts aligning on the dentin surface of lacunae (Figure 3, c). Although some deciduous tooth roots showed mild resorption, cellular cementum covered the scraped dentin surfaces (Figure 3, d).

As is well known, the primary root resorption process is regulated in a manner similar to bone remodeling, involving the same receptor ligand system known as receptor activator of nuclear factor-kappa B/RANK ligand (RANK/RANKL). Its minor part is promoted by upregulation of vascular endothelial growth factor (VEGF) that upregulates the expression of RANK on osteoclast precursors as does M-CSF [28, 74, 76]. The overfilling of root canals results in the acceleration of deciduous tooth resorption. In all experiments with excess paste, the varied degrees of granulation tissue that developed in the periodontium seem to intimately relate to marked root resorption. The number of monocytes which appeared around the tooth germ of a permanent tooth correlates with the number of osteoclasts absorbing the deciduous tooth. The increase in number of monocytes or precursor cells of osteoclasts accelerates bone resorption, which simultaneously relates to the permanent tooth eruption [42, 45, 75].

In this experiment, infiltrated macrophages may have two important roles. The first is as a source of cytokines inducing odontoclasts/osteoclasts and the second is as a precursor of odontoclasts /osteoclasts. Mononuclear precursors of human osteoclasts have been identified in both bone marrow and the circulation. Precursor cells capable of osteoclast differentiation are present in the marrow compartment, the monocyte fraction of peripheral blood, and in the macrophage compartment of extraskeletal tissues, and these cells are capable of differentiating into mature functional osteoclasts [56]. In inflammatory reactions, macrophages play a key role for tissue regeneration and tolerance. Their differentiation is thought to be regulated by macrophage colony stimulating factor (M-CSF)/colony stimulating factor-1 (CSF-1). The ability of macrophages to produce M-CSF secures macrophage differentiation under Th1 and Th2 cells [55]. M-CSF is essential for producing in inflammatory lesions and osteoclast formation, but the participation of inflammatory cytokines in osteoclast differentiation is complex [29, 40, 55]. In addition to M-CSF, interlukin-1$\alpha$ (IL-1$\alpha$), tumor necrosis factor-$\alpha$ (TNF-$\alpha$) and other key molecules take part in the bone resorption and osteoclast differentiation [72, 77]. Excess filler also causes proliferation of granulation tissue composed of fibroblasts, endothelial cells and lymphocytes. Lymphocytes are immune cells that can produce IL-1, IL-6, and IL-17, TNF-$\alpha$ and RANKL [4, 27]. Quinn and his coworkers demonstrated that fibroblasts of extraskeletal tissues, such as skin fibroblast, could express RANKL and M-CSF and support osteoclast formation [57]. Furthermore, IL-1 directly activates RANK signaling other than inducing RANKL to promote osteoclastgenesis [41]. Thus, the area with extruded filler provides the backgrounds for the increasing number of odontoclasts and acceleration of tooth resorption (Figure 4).

### 2)  Increase in number of TRAP-positive multinucleated giant cells by excess filling paste

Controls and experiments without overfilling show scattered tartrate resistant acid phosphatase (TRAP)-positivity, and flattened mononuclear cells on the surface of cementum without resorption 2 weeks after treatment (Figure 5, a). At 4 and 8 weeks, TRAP-positive cells were slightly increased in number.

Excessively filled cases showed that mononuclear cells and MGCs appeared in the periodontal tissue, accompanied by flattened or dendritic TRAP-positive cells on/close to the
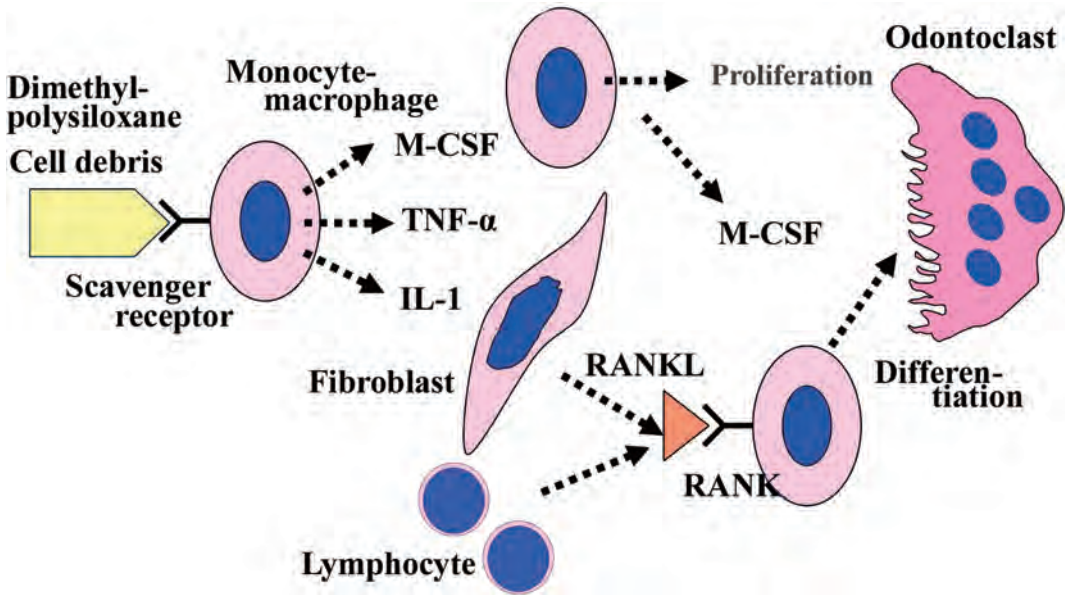
**Figure 4**    Activation of odontoclastgenesis: M-CSF, TNF-α and IL-1 induce the monocyte proliferation or RANKL production, consequently accelerating tooth resorption.

root surface 2 weeks after operation. Foamy mononuclear cells and some MGCs having large vacuoles did not demonstrate TRAP activity. However, other MGCs containing phagocytotic vacuoles showed a weak TRAP activity in part. The intensity of TRAP activity varied from cytoplasm to cytoplasm (Figure 5, b and c). In the distant periodontal tissue from the root apex with the overflowed filling paste, mononuclear cells and multinuclear cells with a weak TRAP-positivity increased in number (Figure 5, d). After 4 and 8 weeks, increased lacunae contained odontoclasts with strong TRAP activity, while mononuclear cells and MGCs surrounding the paste showed somewhat weak and variable reactions to TRAP, the as same as that in two-week cases.

Bone marrow macrophages show TRAP activity in certain pathological conditions such as chronic leukemia, metastatic cancer, excess transfusion, osteomyelodysplasia after chemotherapy, and so on. Therefore, TRAP is considered as a marker of cell activity rather than of cell differentiation [10]. Giant cell tumor of bone contains not only TRAP strongly positive MGCs but also TRAP weakly positive macrophage-like cells [46]. In experimental cases with excess filler, preodontoclast-like multinuclear giant cells as well as FBGCs with vacuoles demonstrated a weak TRAP positive reaction. These two types of giant cells can be divided by the extent of reaction. However, this result suggests that TRAP reaction is not a specific marker of osteoclasts/odontoclasts. A TRAP appears to reflect the phagocytotic activity or function of these cells rather than their differentiation. Osteoclasts/odontoclasts have numerous mitochondria, cytoplasmic vacuoles and lysosomes similar to mature macrophages and FBGCs [14]. In another example, extraskeletal or giant cell tumors of soft tissue show the same histological and immunohistochemical characteristics as giant cell tumors of bone, that is, osteoclastoma [26]. Concerning the immunophenotypic character, osteoclasts share the same membranous antigens with both macrophages and FBGCs [7, 56], which shows a similarity among these cells. Of this in vivo examination, the results suggest that FBGC can phagocytize dental hard tissue in certain pathological conditions; details of the findings will be described in
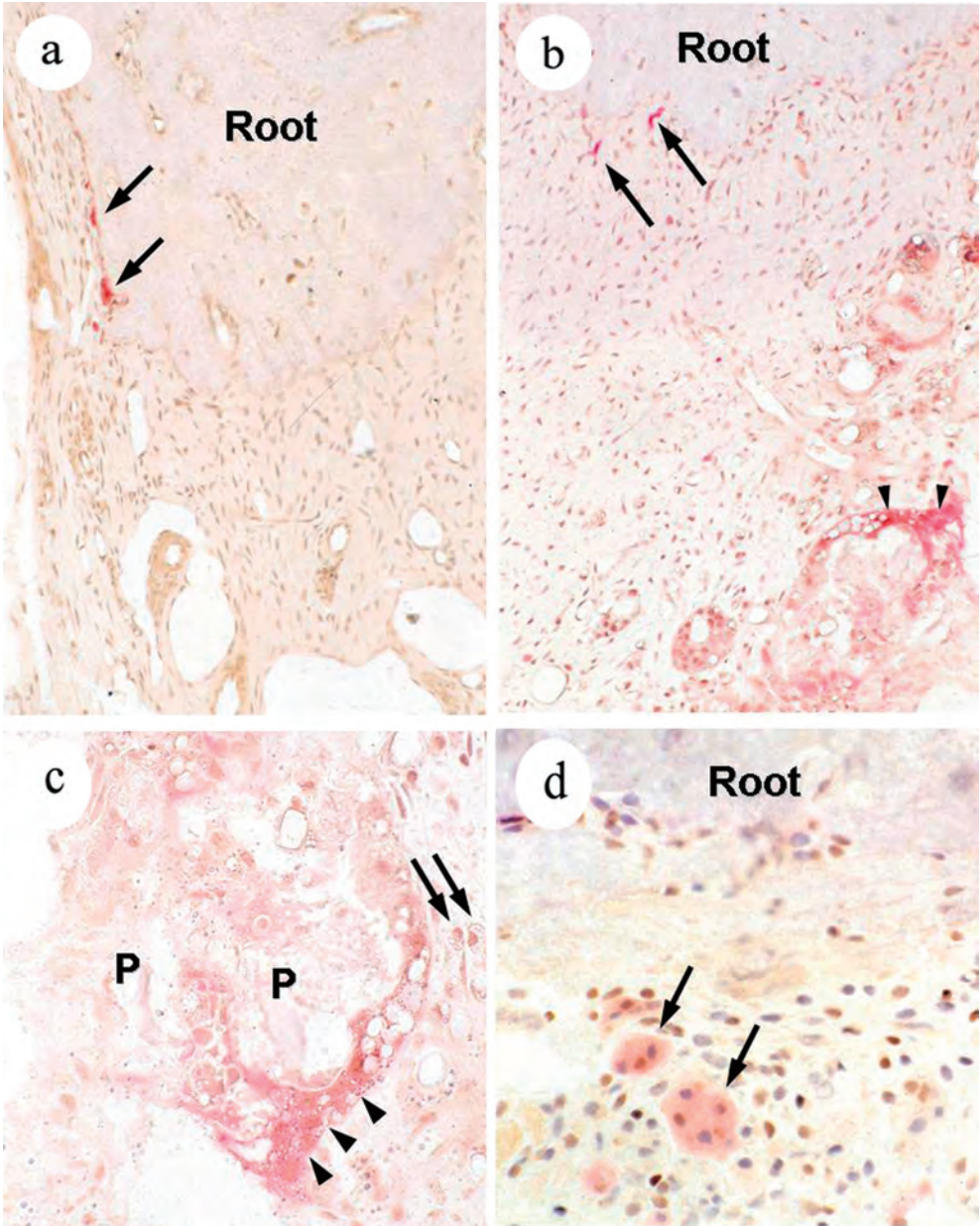
**Figure 5**    TRAP staining features counterstained with hematoxylin

a:  A TRAP activity is detected in the cytoplasms of mononuclear cells laying on the cementum surface without resorption in a 2-week-control.

b:  In a 2-week experimental case, TRAP-positive-dendritic cells (arrows) are recognized. Moreover, multinucleated giant cells are phagocytizing the excess paste in the periodontium.

c:  This photomicrograph is a high-power view of Fig. 5, b. A multinucleated giant cell is positive for TRAP staining (arrowheads), but negative for foamy mononuclear cells (arrows).

d:  In the distant periodontium from the root apex with overfilling, there are proliferating mononuclear cells and multinuclear cells with a weak TRAP-reaction (arrows).

the following sections. Detection of TRAP positivity on FBGCs is an interesting phenomenon that shows the cell activity or function seems to change according to the kinds of foreign bodies or the periods of reactions. On the other hand, a well-developed ruffled border and strong TRAP reaction of odontoclasts could show extremely stronger phagocytotic activity than that of FBGCs.

The environment might significantly affect the function which a multinuclear giant cell could obtain. Whether FBGCs can alter their character is discussed on *in vivo* experimental models using rat subcutaneous tissue in parts 2 and 3 of this chapter.
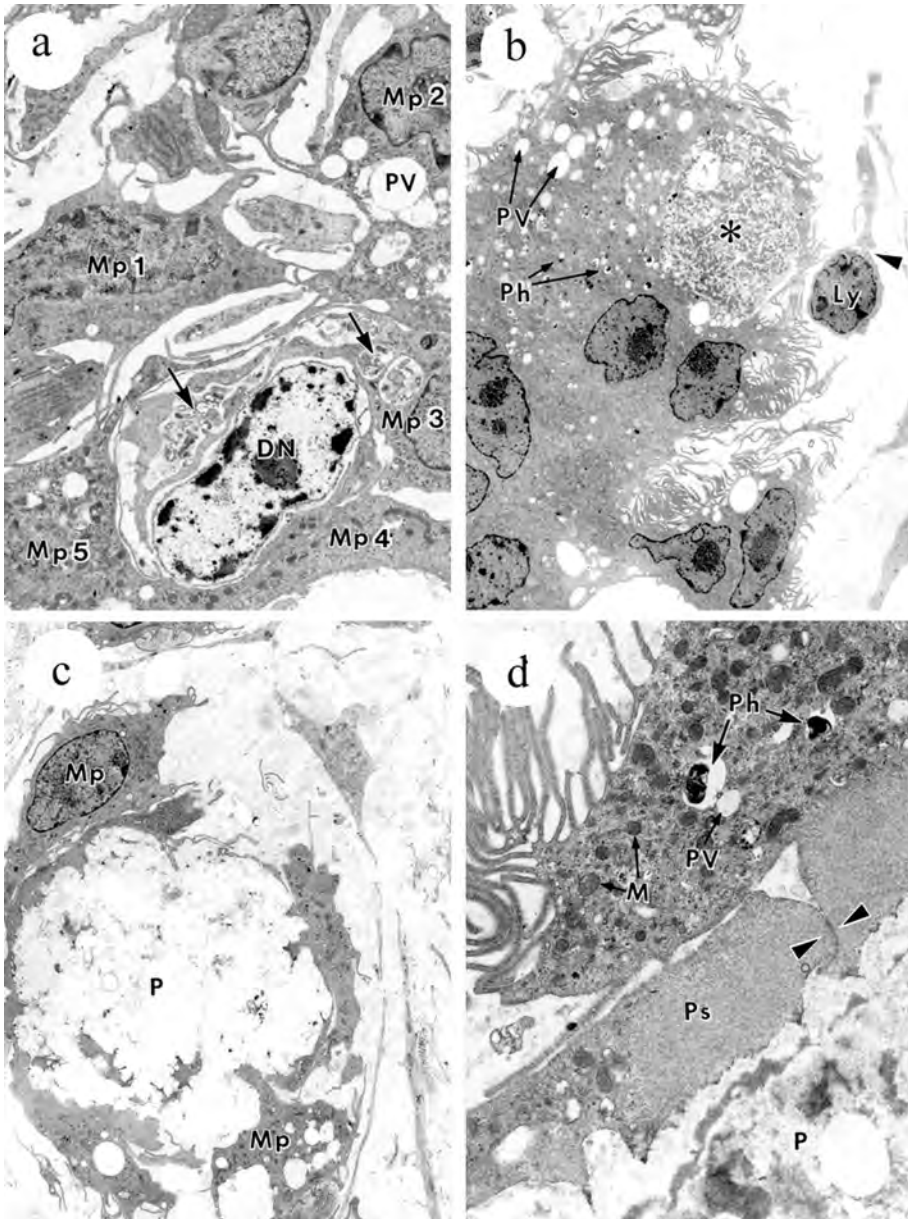
### 3) Formation of multinucleated giant cells by overflowing filling paste

As described above, the excess paste that flowed out into the periodontal tissue was surrounded by granulation tissue composed of mono- and multinuclear cells. Numerous macrophages infiltrated around the overfilled paste 4 weeks after the operation. In electron microscopic photographs, the overflowing paste was mostly observed as spaces so that the paste mostly disappeared during the preparation of tissues. Sometimes, delicate, moderate electron-dense microfibrils with reticular structure remained in the peripheral areas of the spaces. Cytoplasms of macrophages facing the paste showed scanty organelles and relatively short and thick processes extending into the paste. Macrophages were most frequently observed 4 weeks after the operation. In this stage, the granulation tissue, predominantly composed of macrophages, proliferated in a granuloma-like fashion. Macrophages, measuring 5 to 20$\mu$m in diameter, phagocytosed medium electron dense substances and these complexly contacted and/or combined with adjacent cells by their long-elongated cytoplasmic processes. Macrophages with phagocytic vacuoles scattered throughout the tissue distant from the excess paste. Mitotic figures were frequently observed in the cells arranged in a cobblestone appearance (Figure 6, a).

Macrophages which phagocytosed the excess paste were widely distributed throughout peripheral nerve tissue observed in places distant from the periapical tissue with extruded paste. Roughly 1$\mu$m-diameter nerve fibers, running sparsely or fascicularly, showed phagocytic and regenerative appearances (Figure 6, b). Nuclei of macrophages infiltrating around the roots were large and irregular. Chromatin was sparsely scattered throughout the nuclei, but heterochromatin was distributed in the periphery. Most macrophages showed that their cytoplasms contained numerous mitochondria, vesicles and phagocytotic vacuoles. Some macrophages with poor organelles were somewhat immature. In the intercellular spaces between proliferating macrophages, there were necrotic cells, degenerated nuclei and organelles as well as much debris irregularly invaded by elongated cytoplasmic processes of macrophages (Figure 7, a). Irregular MGCs were also noted in the periodontal tissues. These MGCs had prominent cytoplasms with well-developed Golgi apparatus, numerous mitochondria and phagolysosome/phagocytic vacuoles. Some macrophages contained a huge phagocytic vacuole which was made up of accumulation of organelle-like reticulum measuring 20$\mu$m in diameter. This macrophage extended a long and slender cytoplasmic process or a villous process whose expanded tip contacted with an adjacent lymphocyte (Figure 7, b). The extruded paste was distributed in small clusters around the root apex. These clusters were observed as spaces containing cell debris and amorphous or granular substances. Long spindle-shaped macrophages with irregular processes surrounded these spaces (Figure 7, c). These macrophages had numerous mitochondria, phagolysosomes and phagocytic vacuoles in their cytoplasm, but the cytoplasm facing the paste or connecting with each other showed poor organelles (Figure 7, d). In this manner, it enclosed the clusters of overflowed filling paste or seemed gradually to
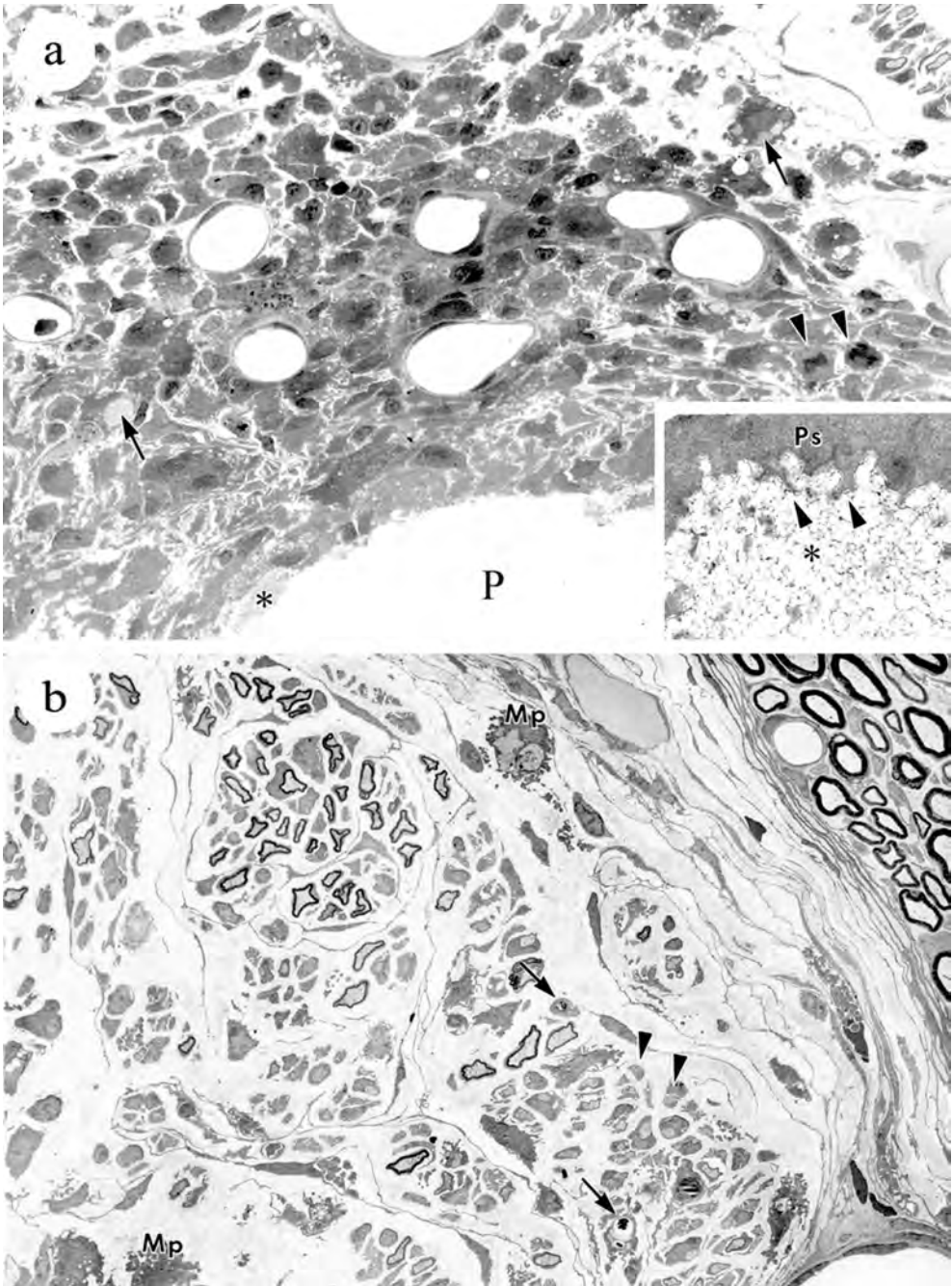
**Figure 6**     Macrophages infiltrating around the overfilled paste 4 weeks after the operation

a:  The area where the excess paste flows out is observed as a space (P). In this space, a small amount of the medium density material (asterisk) is noted. Numerous macrophages contain vacuoles (arrows) of various sizes and some of them show a mitotic figure (arrowheads). Inset: Macrophages extend pseudopodia to the micro-filamentous material (asterisk).

b:  Macrophages (Mp) containing droplets scatter throughout the nerve fivers that show phagocytosis (arrows) and regeneration (arrowheads) of neurofilaments in the peripheral tissue of the overflowed paste (P).

**Figure 7**    Multinucleated giant cell formation 2 weeks after the operation

a:  The nucleus and organelles (arrows) of degenerated cell (DN) are surrounded by macrophages (Mp1-Mp5) that have phagocytic vacuoles (PV). But some macrophages show scanty cytoplasms.

b:  A large phagocytic vacuole contains the structure suspected as accumulated endoplasmic reticula (asterisk) in the multinucleated giant cells with numerous phagocytic vacuoles (PV) and phagolysosomes (Ph). Note a lymphocyte (Ly) contacts with a multinucleated giant cell by an elongated process (arrowhead).

c:  Some macrophages (Mp) enclose the overflowed paste.

d:  Cytoplasms facing the paste (p) show scanty organelles. Pseudopodia (Ps) or cytoplasmic processes surrounding the paste connect with each other (arrowheads). M: mitochondria, Ph: phagolysosome, PV: phagocytic vacuole

transform into MGCs.

MGCs enclosing the paste were variable in shape. These showed flattened cytoplasms and a reticular fashion in part. The cytoplasms had numerous mitochondria and phagolysosomes, but relatively scant phagosomes. Reticular cytoplasms combined with their villous cytoplasmic processes or connected with macrophages (Figure 8, a). Some MGCs surrounded the space in an almost ring-like fashion. The external cytoplasmic membrane had irregularly extended processes, but the internal surface of the ring-like cytoplasm was smooth. The spindle nuclei with irregular nuclear membranes were situated in the periphery of the cytoplasm. Furthermore, the circular giant cells connected with the cells with mitotic figures, which expanded their cytoplasm to completely enclose the excess paste (Figure 8, b).

As clearly demonstrated by this study, the tissue reaction to excessively overfilled paste results in proliferation of granulation tissue that is composed of foamy macrophages and MGCs after 2 weeks. This reaction is also derived when the paste enters the periodontal tissue after tooth absorption in the cases with adequate root canal filling. Electron microscopic observations disclosed that this reaction is similar to the formation of epithelioid granuloma [3]. Four weeks after the operation, the paste was surrounded by a proliferation of mature macrophages, arranged in a cobblestone appearance. At the later stage, the number of infiltrating macrophages appeared unchangeable.

The metabolism of the silicone has been controversial. In this study, macrophages with large phagocytic vacuoles were widely distributed, only in the periodontal tissue, but also in the tissue distant from the root apex. Phagocytic vacuoles of macrophages contained some droplets which seemed to be silicone. Kawakami and his colleagues have reported that silicone embedded in the subcutaneous tissue is detected in macrophages, MGCs, capillaries of originally embedded tissue, and distant cutaneous tissue and digestive organs [35, 36]. A small amount of silicone seems to be excreted in the urine after transition into blood. This examination does show the systemic movement of the paste, but infiltrated macrophages take an important roll in the disposal of the excess paste including silicone oil. The wide movement of macrophages with the paste implies wide distribution of the paste, as well as silicone. The filling paste excessively carried out of the root canal does not stay in the apical periodontium. This is an important problem after the overfilling since some components of the paste remain for at least 8 weeks in the peripheral tissues.

It is thought that MGCs are formed by mitoses without cell division or by cell fusions. Black and his co-workers [14] had been already showed that MGCs arising in the metal granuloma did not divide their cytoplasms through the $^3$H-thymidine labeling method. All of the interdigitation of epithelioid cells did not reveal their cell fusion, but they thought that this feature could explain the formation of MGC and FBGCs, or that Langhans type giant cells could be made by cell fusion. In this model, we can find two types of giant cells: irregular-solid and circular ones. Concerning these features that show macrophages surrounding degenerated cells and the excess paste, accompanied by the connection of neighboring cells, the processes of giant cell formation are estimated to be as follows. The former irregular-solid type giant cell is made by following processes: a) some macrophages surround relatively small particles of the paste or degenerated cell debris; b) neighboring macrophages connect with each other; and c) cell fusion occurs with large phagocytic vacuoles in its cytoplasm. The later circular type giant cell is made by following processes: initially macrophages surround a large amount of the paste and neighboring macrophages connect with each other; finally cell fusion occurs, but the paste remains without phagocytosis. It is well known that macrophages have the scavenger receptor CD36. Recent study suggests that CD36 is required for cytokine-induced fusion of macrophages
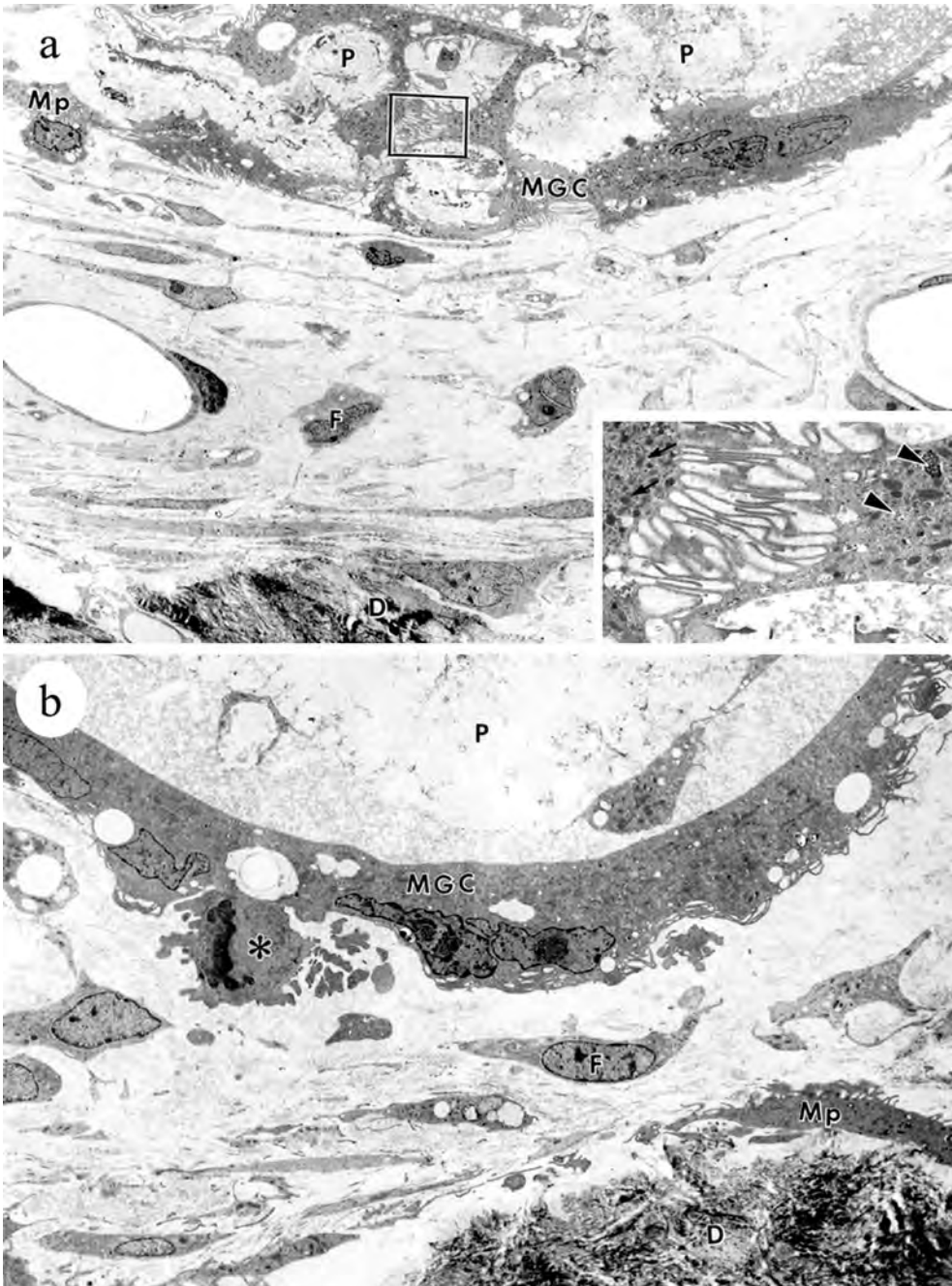
**Figure 8**    Multinucleated giant cell formation 2 weeks after the operation

a:  Giant cells (MGC) surrounding the paste show a reticular structure in part and contact macrophages (Mp). The high power electron micrograph of a rectangular part demonstrates the interdigitation between extending processes from mitochondria (arrows) and phagosome-(arrowheads) rich cells (inset).

b:  Another giant cell (MGC) surrounding the paste shows a ring-fashion. Its cytoplasms contain a few phagosomes and show a smooth internal surface. Note a cell with mitosis (asterisk) connected with this giant cell. D: dentin, F: fibroblast, Mp: macrophage
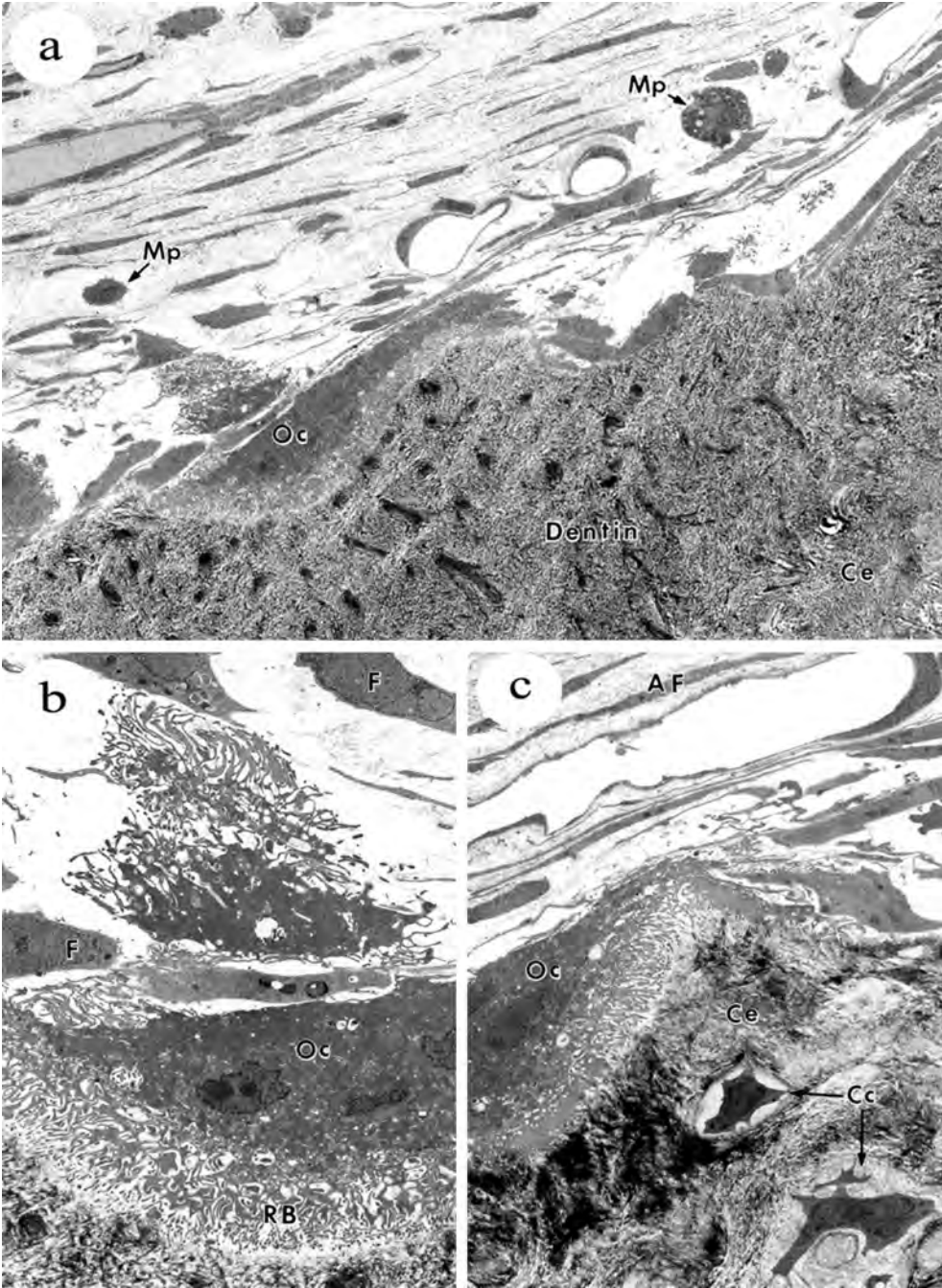
**Figure 9**    Normal appearance of root resorption in the control 8 weeks after the operation

a:  The control without treatments shows the internal and external resorption of the root apex. The pulp tissue of the root canal shows odontoclastic (Oc) dentin resorption, accompanied by infiltration of a few macrophages (Mp). Note remaining cementum in the apex.

b:  A high power field of Fig. 10a shows an odontoclast with well developed ruffled border (RB) and extended cytoplasmic processes in all directions. F: fibroblast

c:  An odontoclast extends its process across the apical constriction and the cementum (Ce).

and is involved in the formation of multinucleated giant cells [31]. Furthermore, circular type giant cell showed mitosis, which might represent the possible feature of MGC formation. It suggests that FBGC made by cell fusion increases its nuclei by mitosis without cell division.

### 4) Tooth resorption via foreign body type giant cells

In the root apices of the controls without treatment, many resorption lacunae were sometimes observed in the pulp, due to internal resorption, even when there was no finding of root resorption. A small number of macrophages and many fibroblasts extending dendritic processes were found within the pulp. However, neutrophils or lymphocytes did not infiltrate. Odontoclasts in the physiologic tooth resorption had a well developed ruffled border and a bouquet of cytoplasmic villi which extended to the center of the pulp. The tooth resorption seemed to develop from the internal dentin to the external cementum of the apical foramen. An odontoclast extended its cytoplasmic process across the apical constriction and absorbed the cementum (Figure 9).

The overfilled cases showed that there were many fibroblasts, macrophages and preodontoclast-like giant cells in the periodontal tissue around markedly absorbed root apices. The dentin surface formed many absorbed lacunae in which mitochondria-rich odontoclasts with a bizarre morphology were situated. These odontoclasts had well-developed ruffled borders (Figure 10, a). The periodontal tissue distant from root resorption developed phagocytosis of collagen fibers by fibroblasts. In these areas, ovoid or irregular-shaped MGCs appeared around capillaries. The cytoplasm of MGCs contained numerous mitochondria, infrequently a centrosome, located in the center of some nuclei. Their cellular surface had numerous micro-villi, accompanied by an irregularly extending cytoplasmic process (Figure 10, b).

In the experimental cases with overfilling, macrophages frequently infiltrated around absorbed roots. Some of them were close to the dentin surface, accompanied by mitotic figures. Giant cells laid their slender cytoplasmic processes on the absorbed dentin surface. Their cytoplasms with numerous mitochondria had phagosomes or vacuoles which contained granular substances. The cytoplasm facing the dentin surface showed scant organelles, which was somewhat similar to the structure of clear zones of odontoclasts. However, these giant cells never had ruffled borders (Figure 11, a). The macrophages covered the absorbed dentin and also showed extending cytoplasmic processes with poor organelles that mimicked clear zones. Collagen bundles of the dentin covered by macrophages showed a characteristic future of fibers loosely arranged in a fluffy fashion (Figure 11, b).

Our experimental model with overfilling showed active root absorption with numerous macrophages and MGCs, but no significant changes were noted in the controls and in those with adequate root canal filling. The experimental phenomenon is thought to be abnormal or an unphysiological reaction due to foreign body reactions. The characteristic reaction to the excess pastes is a significant infiltration of macrophages. We have no doubt that odontoclasts take a main role in root resorption. There is an important relationship between odontoclasts and macrophages in the root resorption with foreign body reactions.

Odontoclasts and osteoclast are thought to be cells of the same linage, but their detail has not been clarified. Osteoclasts are derived from a monocyte-macrophage cell line [7]. It is well recognized that $1\alpha$, 25-(OH) 2D3, RANK- RANKL, and other important signaling pathways participate in osteoclast differentiation. Under the presence of these factors, precursor cells capable of osteoclast differentiation are present in the marrow compartment, the monocyte fraction of peripheral blood, and in the macrophage compartment of extraskeletal tissues. These cells of macrophage-monocytic lineage have the ability to differentiate into mature functional
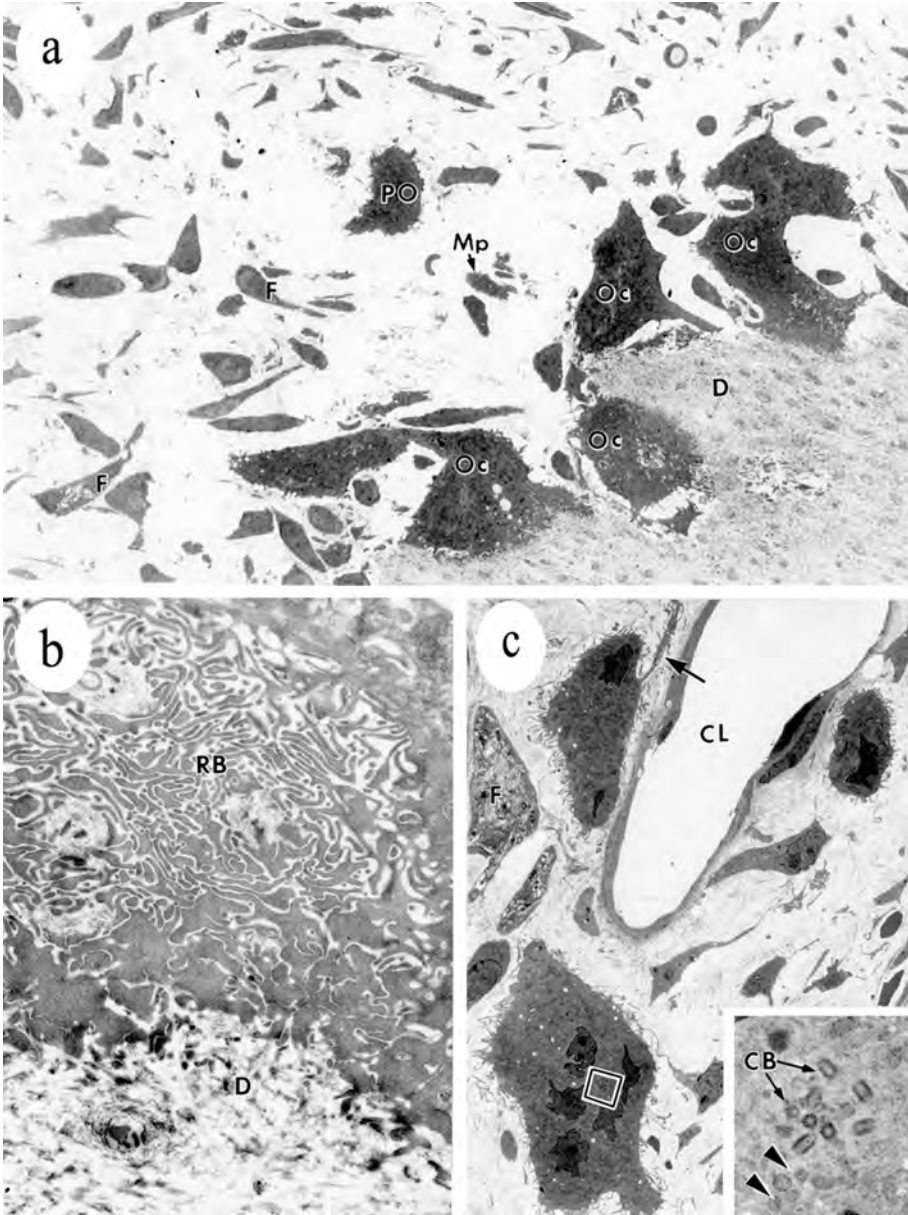
**Figure 10**   Odontoclasts markedly absorbed the deciduous teeth in the experiment, 8 weeks after the operation

a:  The periodontal tissue of an overfilled case shows macrophages (Mp) and preodontoclast-like cells (PO) in addition to periodontal fibroblasts (F). Many odontoclasts (Oc) make resorption lacunae on the dentin (D).

b:  A high power view of odontoclasts (Oc) shows a relatively developed ruffled border (RB) in its structure.

c:  In the periodontal tissue distant from the overfilled area, multinucleated giant cells and fibroblasts (F) phagocytosed collagen fibers around a capillary (CL). This giant cell has microvilli and extends a long cytoplasmic process (arrow). In the rectangular area of multinucleated giant cell, many mitochondria (arrowheads) and the sentrosome or central body (CB) are observed.
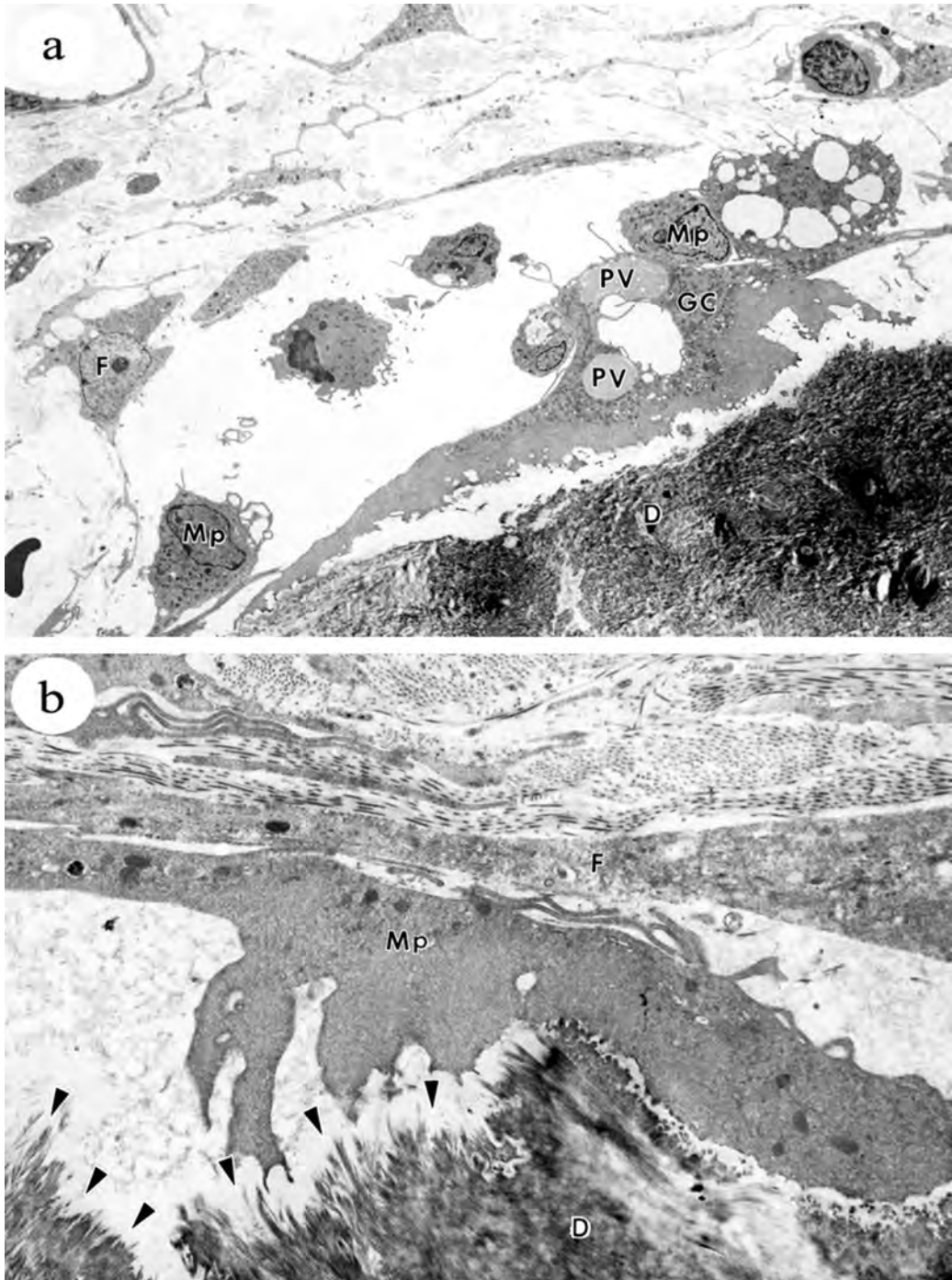
**Figure 11**  Dentin resorption by foreign body giant cells 2 weeks after the operation

a:  In the overfilled case, a giant cell (GC) with large phagocytic vacuoles (PV) lies on the dentin (D) surface. Immature macrophages contact with a giant cell. GC: giant cell, F: fibroblast

b:  Elongated process of a macrophage (Mp) contacting with dentin shows clear-zone like structure of the odontoclast. The collagen fibers of the dentin (D) covered by the cytoplasmic process of a macrophage (Mp) are fluffy or loose (arrowheads).

osteoclasts [29, 58, 70]. Simultaneously, the presence of osteoblasts producing induction factors is necessary for osteoclast differentiation [1]. However, we have insufficient knowledge how physiological root resorption by odontoclasts is controlled. Just after the stable period, numerous fibroblasts and macrophages, which phagocytize collagen fibers, appear in the periodontal tissue of deciduous teeth. Cementoblasts seem to take the same role as that of osteoblasts in odontoclast differentiation [63]. Many pre-odontoclastic MGCs were also seen in the perivascular tissue which is distant from the overfilled area, and which might represent that the cementoblast is not an essential factor to odontoclastic root resorption. Not only skeletal fibroblasts but also extraskeletal fibroblasts such as skin fibroblasts are capable of produce RANKL and M-CSF and supporting osteoclast formation [57] so periodontal fibroblasts act similarly.

The number of odontoclasts appearing around the crown of a permanent tooth correlates with that of monocytes in the tooth exchange of a dog. The increase in the number of monocytes could accelerate the bone resorption, which simultaneously would help permanent tooth eruption [43, 47, 77]. In previous research, fully-developed alveolar macrophages differentiated into odontoclast-like cells whose prevalence related to the number of alveolar macrophages [69]. Odontoclast differentiation from its precursor cells is controlled under the presences of several induction factors such as macrophage colony stimulating factor (M-CSF)/colony stimulating factor 1 (CSF-1), interleukin-1α (IL-1α), tumor necrosis factor α (TNFα), and so on. It is well known that macrophages produce some of them [27, 55, 73]. For example, IL-1α stimulated the formation of osteoclast-like cells via an increase in M-CSF and prostaglandin E2 (PGE2) production, and a decrease in osteoprotegerin (OPG) production by osteoblasts [67]. Concerning these facts, the overflow of the filling paste could result in the increased infiltration of monocytes and macrophages with the production of some cytokines, M-CSF, IL-1α or TNFα,
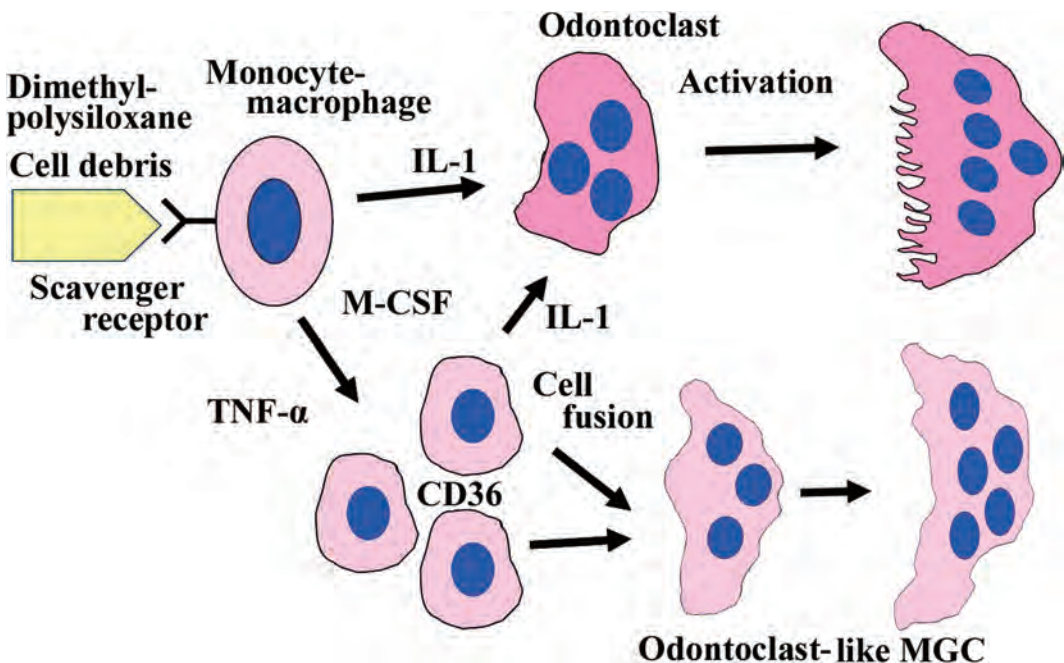


**Figure 12**   Tooth resorption via odontoclast and odontoclast-like foreign body giant cells: Overfilling causes odontoclast activation and odontoclast-like MGC formation that participates in tooth resorption.

which appears to accelerate tooth resorption under the development of odontoclast differentiation in the periodontal tissue with excess paste. Thus, the excess paste makes the local cytokine level up-regulate through the assembly of macrophages and accelerates tooth resorption by both odontoclasts and odontoclast-like giant cells (Figure 12).

Under the physiologic condition, both odontoclasts and macrophages are closely related to root resorption. In fact, dentin fragments are sometimes phagocytozed by macrophages [62] and the exact example will be presented in part 2 of this chapter. Odontoclasts are similar to osteoclasts but their nature is controversial. MGCs appear in various lesions, such as foreign body granulomas or some neoplastic lesions. MGCs arise in giant cell tumor of which neoplastic cells are capable of absorb hard tissue [46]. MGCs of breast caner could absorb bone fragments in vitro. Interestingly, this resorption is directly activated by parathyroid hormone stimulation [8]. In other examples, hydroxyapatite or polymethylmethacrylate particle-associated macrophages are differentiated into multinucleated giant cells with tartrate resistant acid phosphatase (TRAP)-positive reaction [60]. Similarly, *in vivo* phenomena will be presented and discussed about their biological characteristics in part 3. MGCs located on the surface of deciduous roots (Figure 11) have the mitochondria-rich cytoplasms with numerous and various sized phagocytotic vacuoles but lack ruffled borders. This feature shows that these giant cells have not differentiated into odontoclasts. Therefore, this type of giant cell should be called FBGC, closely related to dentin resorption under the excess root canal filling.

## Tooth resorption via experimentally-induced foreign body multinucleated giant cells *in vivo*

As mentioned above, root canal overfilling brought early root resorption both for odontoclasts and foreign body giant cells (FBGCs) *in vivo*. In the examination using deciduous teeth of dogs, the start times of the experiments and the conditions of root canal filling are varied or inconstant. Moreover, it is problematic that odontoclasts arise in physiological root absorption with the eruption of permanent teeth as the background. It was thought that this experimental model was insufficient to clarify the function of foreign body type multinucleated giant cells (MGCs) and the relationship between odontoclast induction and the excess root canal overfilling. Therefore, another experimental model regarded as a root apex was prepared to focus on these problems.

In this model, we performed subcutaneous implantation of root fragments in rats. Under abdominal anesthesia, lower left and right incisors were amputated and shaped into cylindrical teeth fragments measuring 4 mm in length. Root canals of left teeth fragments were enlarged up to size N-40 (Figure 13). Finally, the root canals of these experimental fragments were filled with calcium hydroxide paste without excess or deficiency. The right side fragments were used as controls without root canal treatment. Three days, 1 week, 2 weeks and 4 weeks after implantation in the dorsal subcutaneous tissue, embedded teeth fragments excised with surrounding connective tissue were routinely process for histochemical examination and non-specific esterase activity was detected.

Histologically, 3 days after implantation, pulp cells of controls remained without significant changes. Slight degeneration and inflammatory cell infiltrations were observed in the pulp of controls. Some neutrophilic leukocytes and mononuclear cells infiltrated the connective tissue that surrounded the cut surface of tooth fragments. In this model, these areas were regarded as apical foramen and periodontal tissue (Figure 14, a). Monocytes were highlighted by granular positivity to non-specific esterase. Especially, dark brown granules were observed in the perinuclear area (Figure 14, b). The number of infiltrated mononuclear cells, including non-

**Figure 13**  Tooth preparation for the experiment: An amputated incisor (upper) was shaped into a cylindrical fragment measuring about 4mm in length. The root canal was enlarged to size N-40 (lower).

specific esterase-positive monocytes in experiments, was more than that in controls. Numerous rounds cells infiltrated around a virtual apical foramen. Especially, a lot of polymorph nuclear leukocytes intermingled with mononuclear cells (Figure 14, c and d).

One week after implantation, infiltration of round cells decreased in the surrounding connective tissue that consisted of the fibroblast and the collagenous stroma. Only hyperemic changes still remained in the control group (Figure 14, e). While experimental tissue showed interesting changes in the surrounding tissue at 7 days, polymorph nuclear leukocytes markedly decreased, yet mononuclear cells were prominent. Mononuclear cells with empty cavities were large and small vacuolated or signet-ring like cells that were scattered throughout the surrounding granulation tissue. Moreover, MGCs with irregular-situated nuclei appeared on the dentin surface. However, these giant cells did not begin hard tissue absorption yet at this stage (Figure 14, f).

Two weeks after implantation, almost all inflammatory cells disappeared in the encapsulating connective tissue comprising collagen fibers and some fibroblasts in control sections. The dentin surface displayed mild absorption by MGCs that had poorly morphological characteristics as typical odontoclasts (Figure 15, a). Experimental specimens showed that the paste in root canals somewhat protruded from the virtual apical foramen. The protruded paste was surrounded by granulation tissue (Figure 15, b and c).

Four weeks after implantation, tooth fragments of controls were encapsulated by thin granulation tissue similar to that of controls after 2 weeks. Multiple scalped-shape lacunae were observed on the dentin surface (Figure 15, d). In experiments, clear resorption lacunae on the dentin surface were accompanied by infiltration of mononuclear cells such as monocyte-macrophages and flat MGCs. Numerous macrophages and MGCs surrounding vacuoles were observed around the filling paste. Interestingly, some MGCs were attached to both the paste and the dentin (Figure 15, e). Note Figure 16. Giant cells that were irregular in shape had fine vesicular phagocytotic vacuoles which faced and attached to both dentin and filling paste. As shown in part 1(Figure 11), this MGC had not only small vacuoles but also relatively large ones in its cytoplasm.

The pathological change in the periodontal tissue with excess paste seems to strongly depend on the components of this filler, which contains silicone as a lubricant. About the fate of silicone oil extruded into periodontal tissue, details are given in the previous section. Briefly,
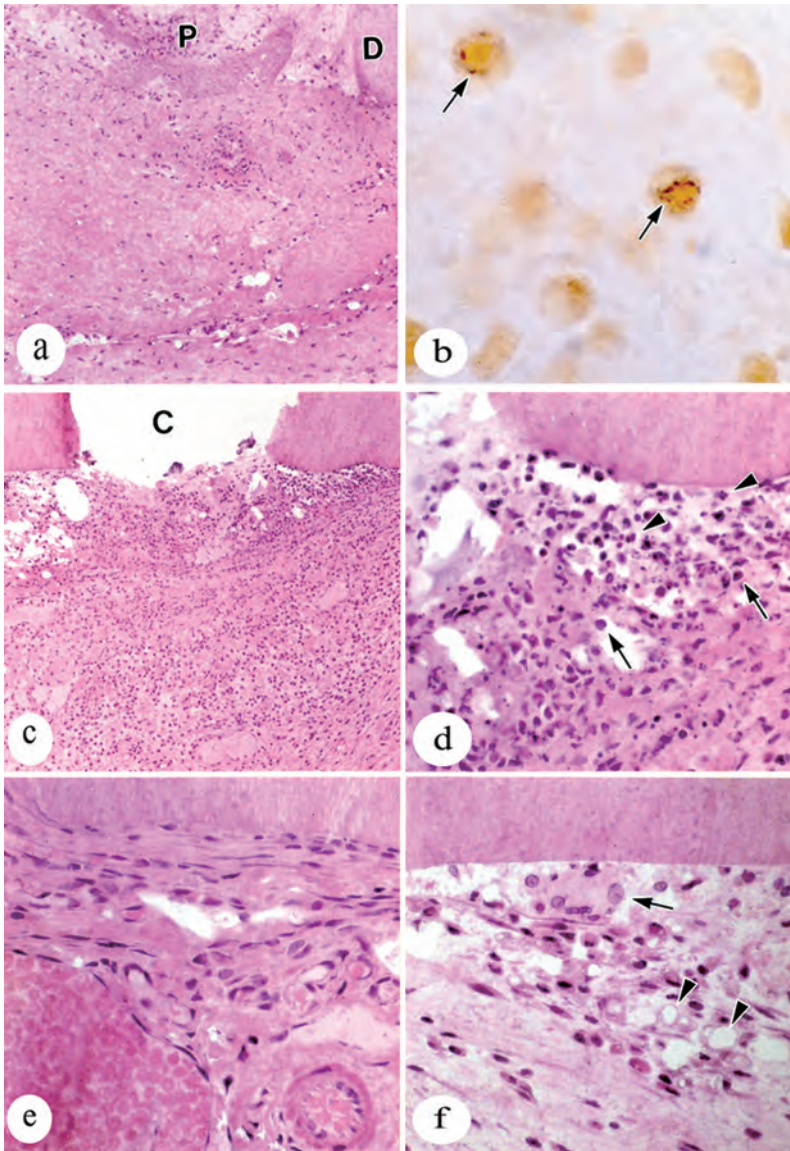
**Figure 14**   Tissue reactions to experimental models

a:  Slight infiltration of round cells are observed in control specimens 3 days after embedding (D: dentin, P: pulp tissue)

b:  Mononuclear cells show granular positive reactions (arrows) to non-specific esterase in controls at 3 days.

c:  Numerous inflammatory cells infiltrate around a filled canal of a left tooth fragment as an experiment after 3 days.

d:  Higher magnification of Figure 14, c shows neutrophils (arrowheads) and monocytes (arrows).

e:  In controls, a few inflammatory cells infiltrate in the granulation tissue encapsulating untreated teeth fragments 1 week after embedding

f:  Multinucleated giant cells (arrow) appeared closed to the cut surface of dentin, accompanied with scattering vacuolated macrophages (arrow heads) in an experimental case.
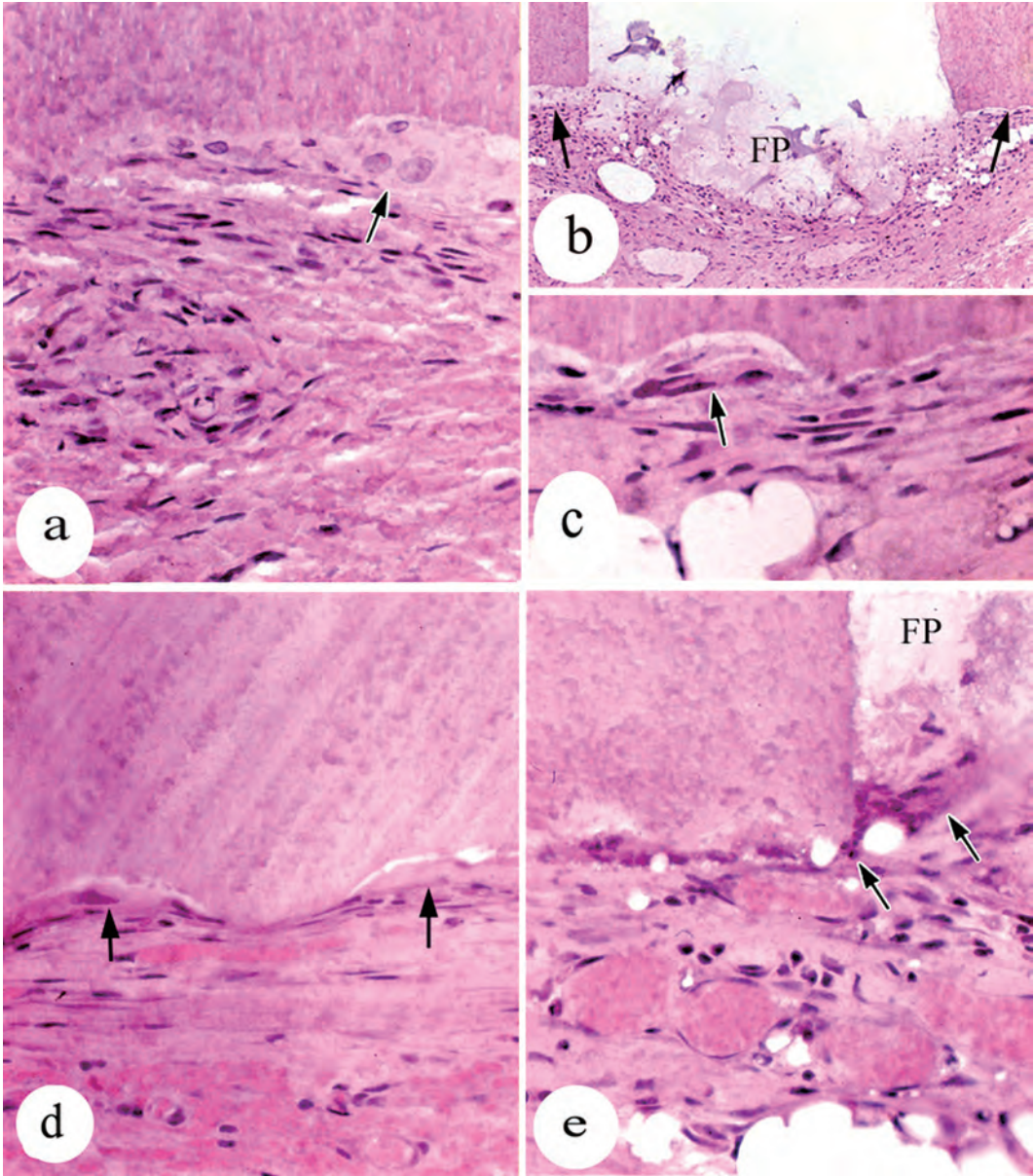
**Figure 15**　Resorption of tooth fragments and filling paste

a: Multinucleated giant cells (arrow) form shallow resorption lacunae in a control.

b: Granulation tissue proliferates around filling paste (FP) in an experiment 2 weeks after implantation. Note resorption lacunae (arrows) of the dentin surface.

c: A high-power view of Figure 15, b shows multinucleated giant cells (arrow) in lacunae.

d: At 4 weeks, giant cells make pits on the dentin surface of a control. A multinucleated giant cell (arrows) lies along both the dentin and filling paste in an experimental case.
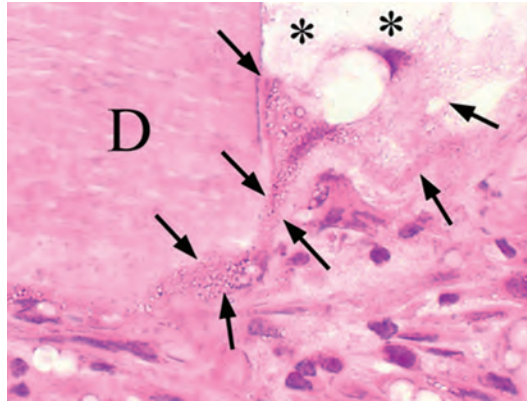
**Figure 16** Multinucleated giant cells with minute vacuoles facing both dentin (D) and filler (asterisks) at 4 weeks.

silicone is hardly absorbed and mainly remains in the local tissue. Some amount of silicone is phagocytozed by macrophages or MGCs, which is well demonstrated in studies using $^{14}$C-labelled silicone oil embedded in rat subcutaneous tissues [34, 36]. The reaction to over filling paste in periodontal tissue is also characterized by infiltration of numerous macrophages and MGCs. MGCs seem to be formed through degenerated or necrotic cells.

Numerous *in vivo* experiments of odontoclasts have been conducted, but many of these are based on models of orthodontic root resorption [16]. This unique experimental model in the rat subcutaneous tissue clearly shows mono/MGCs with cytoplasmic vacuoles around the both ends of a tooth figment, namely, the hypothetical apical foramen. This change seems to be caused by filling paste because it cannot be found in the controls. Acute inflammatory reaction is localized around the virtual foramen and granulation tissue consequently formed in the limited area. In this experiment, because the root canal paste was filled in canals having the same diameter, the cross-section of canals and the contact area between the paste and surrounding tissue was almost equal. Therefore, the extent of granulation tissue that appeared around the virtual apical foramen may be constant. The most impressive feature of this model is the formation of resorption lacunae. 14 days after implantation, lacunae which formed on the surfaces of the virtual root apices were found in both controls and experiments. The precise amount of dentin resorption is unclear from this experiment because quantitative data for both groups are not shown. However, MGCs can be found in experiments but not in controls after 7 days. This result suggests that MGC formation is accelerated by foreign body reaction to root canal filling paste. In fact, there are numerous inflammatory cells observed in experiments in comparison with controls.

Increased inflammatory reaction in experimental cases may serve cytokines more than controls. Interleukin-1$\alpha$ (IL-1$\alpha$) is one of the most potent bone-resorbing factors involved in the bone loss that is associated with inflammation [67]. Macrophages secrete an array of inflammatory mediators following activation. A resting macrophage becomes activated in response to microbial products, immune complexes, chemical mediators, certain extracellular matrix proteins, and T lymphocyte-derived cytokines. Activated macrophages are capable of secreting a wide range of cytokines such as IL-1, IL-6, IL-10, IL-12, IL-18, and TNF-$\alpha$, TGF-$\beta$ TGF A $\beta$-8, MCP-1, and MIP-1$\alpha$/$\beta$ [4]. Activated macrophages play an important role in several pathological conditions such as inflammation and tissue regeneration including foreign body

reaction [55]. In tooth resorption, several cytokines control the induction and function of odontoclasts or osteoclast, and macrophages have a close connection with the control of LI-1 and other cytokine production [1, 53]. Odontoclasts and osteoclasts have the same biological characteristic, which has long been known [22], and both tooth and bone resorption is thought to be regulated in the same manner [28]. Concerning these facts, the increased number of macrophages seems to participate in formation of MGC, odontoclastic tooth resorption and alveolar bone resorption in the shedding process of experimental cases, as described in part 1.

Another interesting finding of this experiment is a MGC of which cytoplasm extends over the resorption lacunae of the embedded tooth and the paste filled in the root canal. This feature might show that the giant cell simply contacts with the paste without phagocytosis. Whether this giant cell can phagocytose the paste was not confirmed because an ultrastructural investigation was not performed in this study. However, this feature is thought to be representative for the nature of MGCs and we believe that these are capable of the processing various materials depending on its environment. In other word, osteoclast is one of specially differentiated foreign body giant cell. Although the exact molecular mechanisms that lead to macrophage fusion have not been fully elucidated, many cytokines such as IL-4 or IL-13 produced in inflammatory foci work as inducers for cell to cell fusion [4]. Therefore, the rat subcutaneous model is suitable for an examination of the functions of extraskeletal or soft tissue foreign body macrophages or odontoclastic giant cells *in vivo*. Further findings of MGCs in soft tissue will be described in the next.

## Characteristics of multinucleated giant cells

Foreign body type and osteoclastic type giant cells cannot be easily divided into two groups. About a hundred year ago [30], multinuclear giant cells (MGCs) were classified into two groups on the basis of their origins: the first group includes MGCs arising in specific tissues such as megakaryocytic, myoblastic MGC and placental trophoblastic giant cells; the second group comprises reactive such as foreign body giant cells (FBGC), Langhans type giant cells of granulomatous inflammation, and osteoclasts. It is generally considered that the former is created through mitoses but the multinucleation of the later is caused by cell fusion. Here, we will discuss the morphological and histochemical characteristics of MGCs that are experimentally induced.

As described parts 1 and 2, certain environments enable MGCs of foreign body giant cells to process various materials, not only dental hard tissue but also biomedical materials for bone regeneration or plastic surgery. Hydroxyapatite (HAP), with an osteoinductive ability, is a non-absorbable and excellent biocompatible material [41, 49], while $\beta$-tricalcium phosphate (TCP) is a bioactive ceramic that is replaced by bone tissue after degradation [49]. Bovine bone particle (BP) that is a deproteinized, as well as sterilized bone particle for artificial bone grafting, has an osteoinductive effect. There are many reports on tissue reactions of calcium phosphate ceramics embedded in rat subcutis [20, 54, 65], soft tissue [19, 48] or bone tissue [19, 20, 23, 39, 41, 49, 52, 54, 66] and *in vitro* experiments [21, 37]. HAP and TCP have been frequently applied to bone augmentation and sinus lift surgery prior to dental implantation. MGCs induced by HAP implantation in periodontium show features similar to osteoclasts, including ruffled borders and clear zones and tartrate-resistant acid phophatase (TRAP) activity [33, 52].

Figure 17 shows an example of sinus augmentation surgery using a bone graft mixture with $\beta$-TCP granules. In this pathological condition, MGCs seem to play an important role in processing of embedded hard tissue particles. Our experimental model for soft tissue MGCs could clarify characteristics of MGCs as follows.
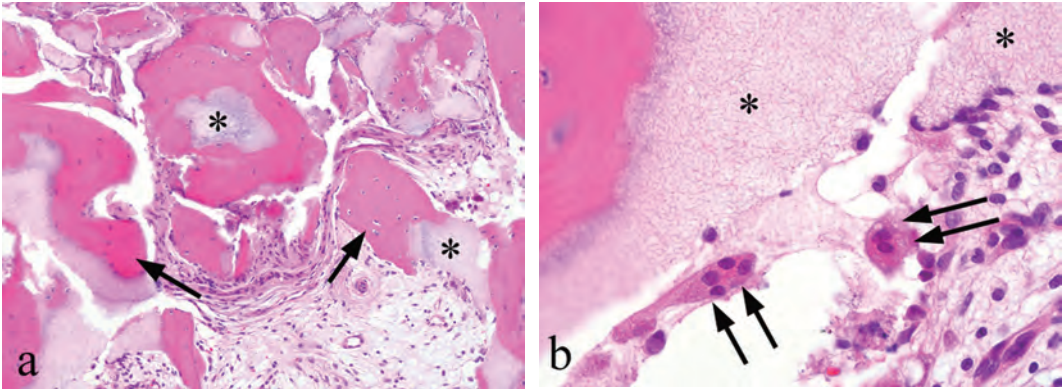
**Figure 17**　Pathological changes of a bone graft mixture in a sinus augmentation surgery four months after the operation

a:　$\beta$-tricalcium phosphate granules (asterisks) remain in regenerated tissue with newly developed bone trabeculae (arrows).

b:　A high-power view of some multinucleated giant cells (arrows) appears close to embedded $\beta$-tricalcium phosphate granules (asterisks).

　　Briefly, four kinds of materials — hydroxyapatite (HAP), $\beta$-tricalcium phosphate (TCP), baked particles of bovine bone (BP) and cholesterin crystals (CHOL) — were milled to diameters of less than 20 $\mu$m and embedded in subcutaneous tissue of anesthetized rats. Three days, 1 week, 2 weeks 3 weeks and 4 weeks after operation, excised samples fixed with 0.1M cacodylate buffered 1. 25% glutaraldehyde 1% paraformaldehyde fixative mixture were embedded in Technovit7100® (Kulzer, Germany) with or without decalcification using 10% EDTA solution (pH7.0). Decalcified or undecalcified 5 $\mu$m-thick sections were histologically and enzyme-histochemically investigated. Enzyme-histochemical characteristics of the MGCs were analyzed as the positive-area ratio of cells reacting positively to non-specific esterase (NSE), acid phosphatase (ACP), tartrate-resistant acid phosphatase (TRAP), and ACP pretreated with cyanuric chloride (CCAP); and TRAP samples with the same pretreatment (CCTP) were measured by means of a color image analysis system. TRAP and CCAP activities were used as osteoclastic markers [47, 50, 71].

### 1) MGCs induced via HAP embedding

　　Microscopically, the embedded HAP was observed as nodules with infiltration of oval or irregular-shaped mononuclear cells. Immature or capillary-rich granulation tissue proliferated around the embedded material (Figure 18, a). MGCs were scattered in foci with many mononuclear cells. These MGCs showed relatively small cytoplasms having two or three nuclei. After 1 week, the implanted area showed aggregation of mononuclear cells within proliferating granulation tissue where oval or irregular-polygonal MGCs with 5 to 10 nuclei had appeared. The number and size of MGCs and the number of nuclei increased compared with the 3 days examples (Figure 18, 2b). Two week cases showed that both mononuclear cells and MGCs increased in number. MGCs had oval or irregular-polygonal cytoplasms showing distinct cell borders compared with that of 1 week samples. Small amounts of HAP particles were observed in their cytoplasms. Relatively large nuclei of MGCs had one or two distinct nucleoli and scanty chromatin (Figure 18, c). In certain parts, many spindle-shaped mononuclear cells were piled up around MGCs and mimicked epithelioid cell features (Figure 18, d). Interestingly, three nuclei
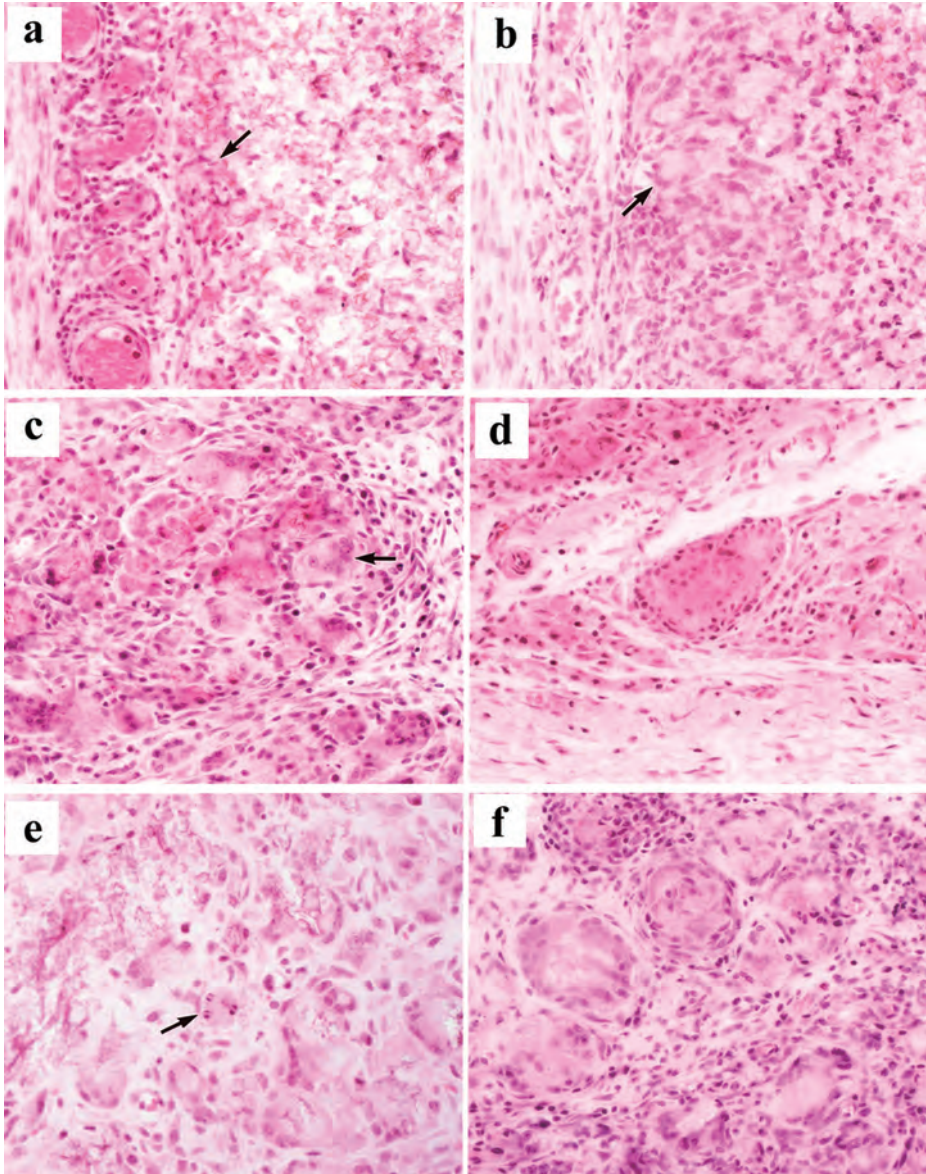
**Figure 18**  HAP group
a:  Mononuclear cells infiltrate around the HAP. Some (arrow) are arranged in like MGC, 3 days after the embedding.
b:  Many MGCs with 5 to 10 nuclei appear, 1 week after embedding.
c:  Most MGCs showing an evident cell border have clear nuclei, 2 weeks after embedding.
d:  Many spindle-shaped mononuclear cells are piled up around MGCs, 2 weeks after the embedding.
e:  Three nuclei simultaneously mitose in a MGC (arrow), 2 weeks after embedding.
f:  MGCs show an increase in size of cytoplasm and the number of nuclei with decrease of embedded granules, 3 weeks after embedding.

of MGCs synchronously showed mitoses (Figure 18, e). The number, size and nuclear number of MGCs had increased more rapidly than those of 1 week samples. Three weeks later, granulation tissue mainly consisted of oval mononuclear cells and MGCs formed nodules. Most MGCs showed similar findings to those of two weeks cases, and their size and number of nuclei were further increased (Figure 18, f). The nuclei of MGCs were often arranged in the periphery of the cytoplasms in the 4 weeks cases. Although their size and the number of nuclei arranged in the periphery of their cytoplasms were quite large, the number of MGCs had decreased (Figure 19, a).

Enzyme-histochemically, positive rates of MGCs and their multiple comparison data in different materials are summarized in Table 1 and 2. Cytoplasms of mononuclear cells were diffuse or granular-positive for NSE (Figure 19, b) but most MGCs were negative. NSE positive reaction appeared at three days and reached maximum reaction at four weeks. Positive reaction of APC was diffuse or granular, infrequently irregular in the cytoplasms of MGCs. Some mononuclear cells were also positive (Figure 19, c). ACP positivity was seen in few cells at three days; it increased after 1 week, reached a maximum at 2 weeks, and then decreased (Figure 20). Similar to ACP, some MGCS and peripherally-situated mononuclear cells showed a strong ACP reaction. There was also a strong and small round positive reaction which was compatible with phagocytic vacuoles of MGCs (Figure 19, d). TRAP activity could not be detected at 3 days but it was observed after 1 week and showed peak reaction at 2 weeks, the same as for ACP. However, the whole positive rate of TRAP was lower than that of ACP (Figure 20). CCAP reaction, which was a relatively weak and diffuse positivity in MGCs and mononuclear cells, was almost similar to the ACP and TRAP reactions (Figure 19, e). In the early stage, namely at 3 days and 1 week, no CCAP reaction was detected but CCAP activity increased at 2 weeks, then gradually decreased after that (Figure 20). As expected, the positive rate of CCAP was considerably lower than that of TRAP. Also in CCTP, a few MGCs and mononuclear cells showed diffuse cytoplasmic reaction that was only observed in 2 and 3 weeks cases (Figure 19, f). The positive rate at 2 weeks was higher than that at 3 weeks, and the CCTP rates were the lowest of all enzyme activities. There was no difference between morphological characteristics of positive and negative MGCs (Figure 20).

### 2) MGCs induced via $\beta$-tricalcium phosphate (TCP) embedding

Three days after embedding, TCP was localized in nodules, and those nodular lesions were encapsulated by immature granulation tissue (Figure 21, a). Most TCP was observed as a large mass but some showed granules of varied sized surrounded by infiltration of oval mononuclear cells in certain parts (Figure 21, b). A large TCP mass was infiltrated by mononuclear cells having swollen and foamy cytoplasms that occasionally demonstrated mitoses (Figure 21, c). At 3 days, MGCs with 2 or 3 nuclei were infrequently scattered in some parts. However, at 1 week, there were a few irregular TCP granules surrounded by many mononuclear cells that occasionally showed MGC-like features. There were numerous MGCs that had about 10 nuclei arranged in the periphery of cytoplasms like Langhans type giant cells (Figure 21, d). After 2 weeks, the number of MGCs, showing distinct cell borders was slightly reduced, but the size and nuclei of MGCs augmented the MGCs in contrast to those at 1 week. Mononuclear cell infiltrates decreased in number and some spindle mononuclear cells piled up around MGCs. (Figure 21, e). MGCs after 3 weeks showed the same histological feature as after 2 weeks, but their size and the number of nuclei had considerably increased (Figure 21, f). Four weeks after the embedding, large MGCs were intermingled with the small MGCs observed at 1 or 2 weeks. Large MGCs, especially measuring over 200 $\mu$m in diameter, were surrounded by lamellarly-
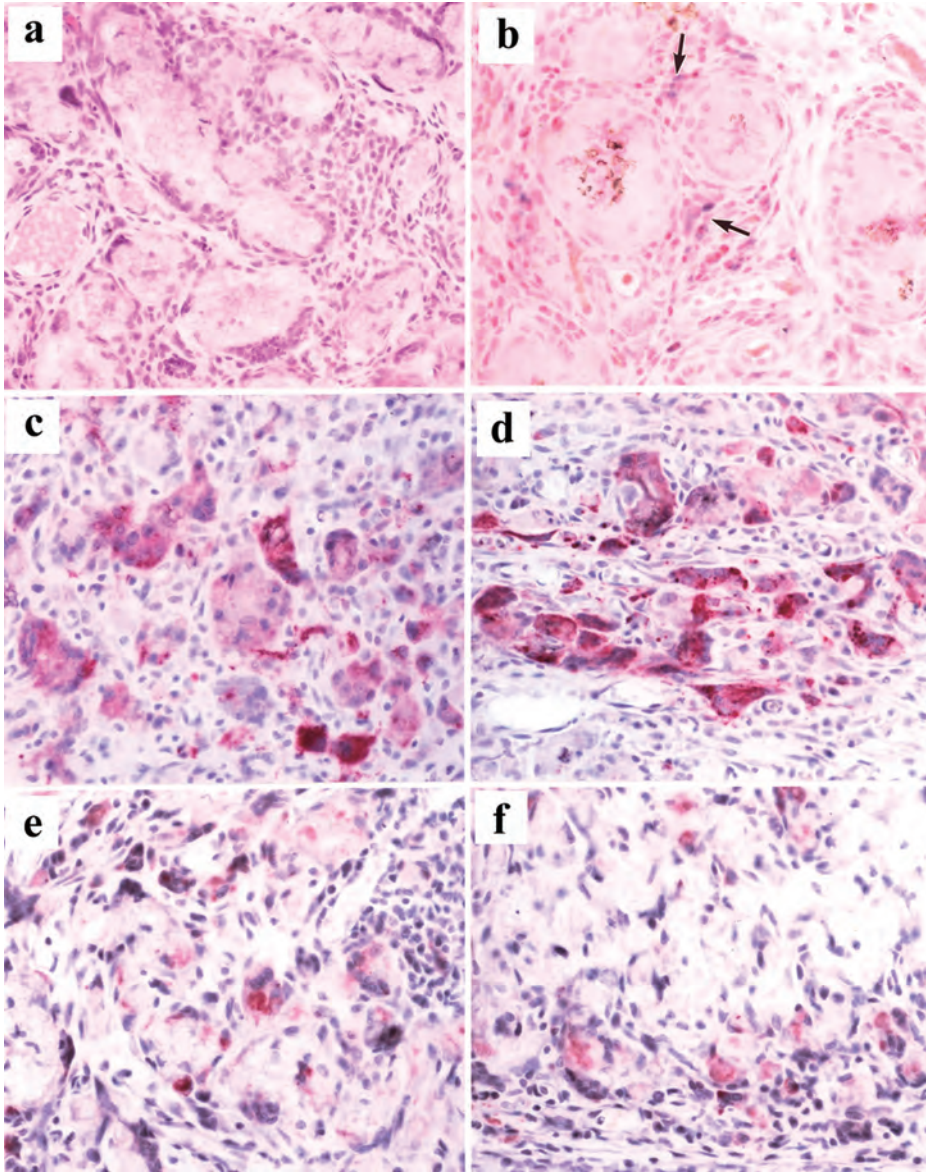
**Figure 19**   HAP group

a:  Many nuclei of MGCs are lined with the periphery of the cytoplasms, 4 weeks after embedding.

b:  Mononuclear cells are positive for NSE (arrow), but MGCs are negative, 4 weeks after embedding, NSE.

c:  Mononuclear cells around MGCs show a strong positive reaction for ACP, 2 weeks after embedding. ACP.

d:  Mononuclear cells around MGCs are strongly positive for TRAP like ACP, 2 weeks after embedding. TRAP.

e:  Diffuse positive reactions to CCAP, like both ACP and TRAP, 2 weeks after embedding. CCAP.

f:  Relative weak reaction is noted similar to CCAP, 2 weeks after embedding. CCTP.

**Table 1**    Positive rate of various enzyme activities in HAP group

|  | 3 days | 1 week | 2 weeks | 3 weeks | 4 weeks |
|---|---|---|---|---|---|
| NSE | 0.32 ± 0.013 | 1.24 ±  0.083 | 1.48 ± 0.065 | 2.90 ± 0.039 | 4.25 ± 0.062 |
| ACP | 0.03 ± 0.011 | 5.53 ±  0.365 | 15.76 ± 0.877 | 13.05 ± 0.441 | 9.70 ± 0.295 |
| TRAP | 0 | 1.12 ±  0.043 | 11.24 ± 0.308 | 8.05 ± 0.203 | 5.57 ± 0.328 |
| CCAP | 0 | 0 | 1.33 ± 0.158 | 0.14 ± 0.036 | 0.02 ± 0.010 |
| CCTP | 0 | 0 | 0.56 ± 0.065 | 0.01 ± 0.0001 | 0 |

(Average ±Standard error ;    n=80, N=2000)

**Table 2**    Multiple comparisons using Scheffé's method of positive rates in HAP group

【NSE】

| 559.92** | 327.93** | 279.42** | 65.98** | 4 weeks |
|---|---|---|---|---|
| 241.49** | 99.72** | 73.84** | 3 weeks | |
| 48.26** | 1.94NS | 2 weeks | | |
| 30.85** | 1 week | | | |
| 3 days | | | | |

【ACP】

| 47.93** | 8.90** | 18.87** | 5.77** | 4 weeks |
|---|---|---|---|---|
| 86.98** | 29.01** | 3.77** | 3 weeks | |
| 126.95** | 53.67** | 2 weeks | | |
| 15.52** | 1 week | | | |
| 3 days | | | | |

【TRAP】

| 77.64** | 49.44** | 80.74** | 15.48** | 4 weeks |
|---|---|---|---|---|
| 162.72** | 120.25** | 25.51** | 3 weeks | |
| 316.72** | 256.44** | 2 weeks | | |
| 3.17* | 1 week | | | |
| 3 days | | | | |

【CCAP】

| 0.01NS | 0.01NS | 40.03** | 0.36NS | 4 weeks |
|---|---|---|---|---|
| 0.47NS | 0.47NS | 32.78** | 3 weeks | |
| 41.13** | 41.13** | 2 weeks | | |
| 0  NS | 1 week | | | |
| 3 days | | | | |

【CCTP】

| 0  NS | 0  NS | 44.01** | 0.001NS | 4 weeks |
|---|---|---|---|---|
| 0.001NS | 0.001NS | 43.85** | 3 weeks | |
| 44.01** | 44.01** | 2 weeks | | |
| 0  NS | 1 week | | | |
| 3 days | | | | |

**:p<0.01
* :p<0.05

arranged mononuclear spindle cells with indistinct cell borders (Figure 22, a).

Enzyme-histochemically, positive rates of MGCs and their multiple comparison data in different materials are summarized in Table 3 and 4. NSE activity of the TCP group was the same as that of the HAP group; namely, it was a diffuse cytoplasmic-positive reaction in the mononuclear cells but negative in almost all MGCs (Figure 22, b). NSE activity was very weak
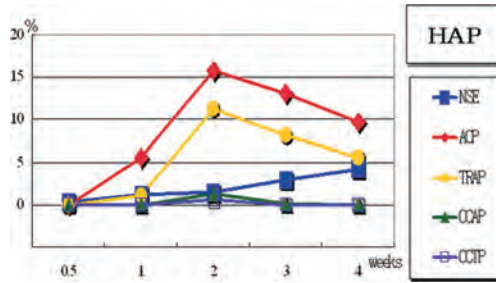
**Figure 20**   Time course of positive rate changes in enzymatic activities after embedding HAP

at 3 days, gradually increasing intensity and reaching peak intensity at 4 weeks (Figure 23). ACP stain demonstrated diffuse or fine-granular reactions in mononuclear cells and MGCs, especially strong activity in the cytoplasms of MGCs which directly attached to embedded TCP granules. Impressive positive reaction was seen as wavy lines surrounding TCP (Figure 22, c). The time course of ACP reaction showed that the activity was not found at 3 days; it gradually increased after 1 week and reached a maximum at 3 weeks, but decreased at 4 weeks (Figure 23). Although the activity of TRAP was very similar to that of ACP, the reaction of TRAP was considerably weak and diffuse, which was restricted in some parts of cytoplasms of mononuclear cells and MGCs (Figure 22, d). The number of positive MGCs was fewer than that of ACP, but the time courses of TRAP and ACP showed similar curves (Figure 23). CCAP activity was also weak-diffuse or fine-granular reaction in some parts of the cytoplasm of MGCs adjacent to TCP and a few mononuclear cells. CCAP-positive cells were very few compared with APC and TRAP (Figure 23, e). Low CCAP activity was only observed at 2 and 3 weeks but not during other periods. The activity was somewhat higher at 3 weeks (Figure 23). CCTP activity was closely similar to CCAP. Diffuse positive reaction was infrequently seen in small parts of cytoplasms of MGCs and a few mononuclear cells situated around MGCs (Figure 22, f). The curve of the time course of CCTP activity slightly rose at 2 and gently reached the top at 3 weeks (Figure 23). There was no morphological difference between positive and negative MGCs.

### 3) MGCs induced via of bovine bone particle (BP) embedding

In Hematoxylin and Eosin staining of BP, embedded materials were observed as a large mass that was the aggregating of bone fragments and aggregation of scattered materials in some parts as well as materials in bone clusters in other parts after 3 days. Oval mononuclear cells infiltrated around bone fragments with some small MGCs that had 2 or 3 nuclei in their cytoplasms showing indistinct cell borders (Figure 24, a). After 1 week, scatted small fragments were phagocytozed by mononuclear cells, while relatively small masses were surrounded by MGCs. Large bone masses were infiltrated by numerous oval or spindle shaped mononuclear cells and MGCs having about 10 nuclei. Infiltrating cells mostly showed indistinct cell borders (Figure 24, b and c). After 2 weeks, large and irregular MGCs phagocytosed small bone fragments within their cytoplasms. Spindle shaped mononuclear cells aggregated and piled up around MGCs with 20 to 40 nuclei (Figure 24, d). In part, spindle cells, gathering around MGCs, showed mitotic figures (Figure 24, e). MGCs, showing the same findings as those at 2 weeks, were becoming distinct cell borders at 3 weeks. Nuclei arranged in the periphery were flattened, but those located near the center were round and clear (Figure 24, f). Although the 4 week
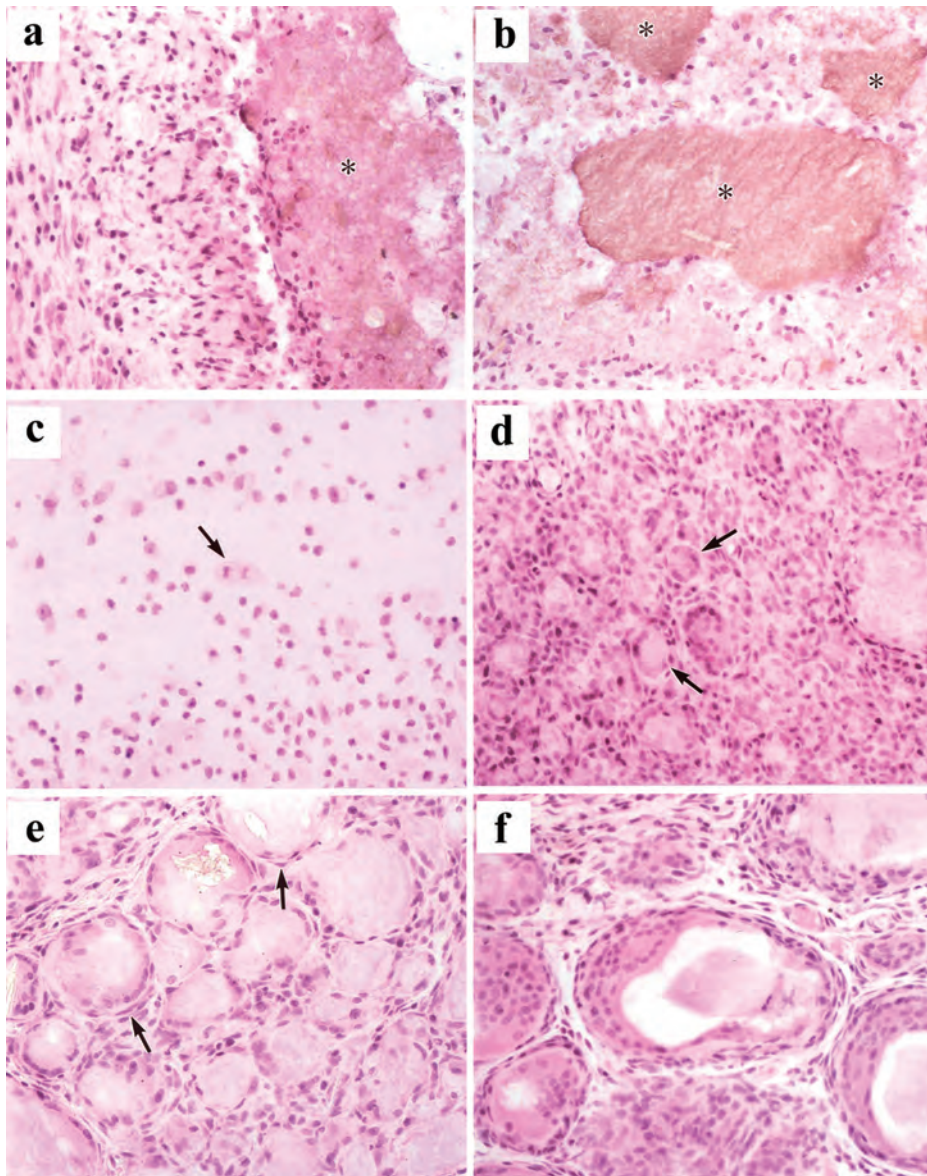
**Figure 21** TCP group

a: Mononuclear cells infiltrate around TCP (asterisk), 3 days after embedding.

b: Mononuclear cells infiltrate between granules of TCP aggregates (asterisks), 3 days after embedding.

c: Scattered mononuclear cells with mitosis (arrow), 3 days after embedding.

d: Many of Langhans type MGCs (arrows), 1 week after embedding.

e: Mononuclear cells (arrows) are close to MGCs showing distinct cytoplasmic outline, 2 weeks after embedding.

f: MGCs increase in size and number of nuclei like 2 weeks example, 3 weeks after embedding.
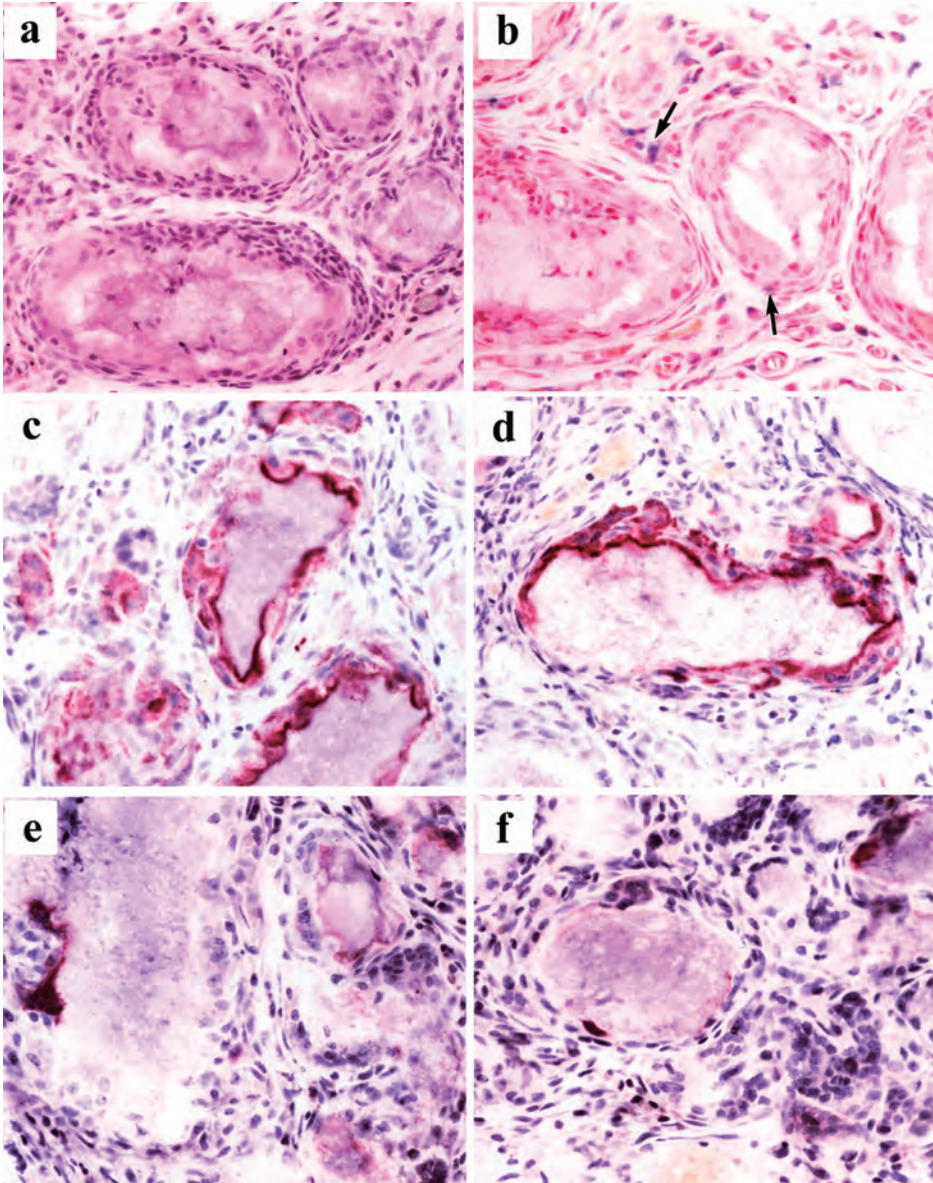
**Figure 22**  TCP group

a:  Numerous mononuclear cells are piled up around large MGCs, 4 weeks after embedding.

b:  NSE positive reaction is found in mononuclear cells (arrows) located around NSE-negative MGCs, 4 weeks after embedding, NSE.

c:  Note NSE positive reactions in both MGCs attached to granular mass and mononuclear cell located in the periphery, 3 weeks after embedding. ACP.

d:  TRAP positive reaction is found as wavy shaped lines surrounding granular masses, 3 weeks after embedding. TRAP.

e:  Faint positive reactions around the granular masses, 3 weeks after embedding. CCAP.

f:  Weak reaction in some mononuclear cells and MGCs, 3 weeks after embedding CCTP.

**Table 3**    Positive rate of various enzyme activities in TCP group

| | 3 days | 1 week | 2 weeks | 3 weeks | 4 weeks |
|---|---|---|---|---|---|
| NSE | 0.24 ± 0.008 | 1.05 ± 0.034 | 2.52 ± 0.063 | 2.64 ± 0.061 | 2.87 ± 0.070 |
| ACP | 0 | 0.46 ± 0.076 | 3.55 ± 0.239 | 8.04 ± 0.706 | 4.66 ± 0.387 |
| TRAP | 0 | 0.20 ± 0.041 | 2.32 ± 0.152 | 4.92 ± 0.613 | 2.11 ± 0.178 |
| CCAP | 0 | 0 | 0.24 ± 0.042 | 0.26 ± 0.08 | 0 |
| CCTP | 0 | 0 | 0.02 ± 0.008 | 0.21 ± 0.046 | 0 |

(Average ±Standard error; n=80, N=2000)

**Table 4**    Multiple comparisons using Scheffé's method of positive rates in TCP group

【NSE】

| | | | | |
|---|---|---|---|---|
| 307.69** | 147.86** | 5.58** | 2.44** | 4 weeks |
| 255.29** | 112.29** | 0.64NS | 3 weeks | |
| 230.42** | 93.01** | 2 weeks | | |
| 28.96** | 1 week | | | |
| 3 days | | | | |

【ACP】

| | | | | |
|---|---|---|---|---|
| 18.81** | 15.28** | 1.26NS | 9.91** | 4 weeks |
| 56.00** | 49.78** | 18.21** | 3 weeks | |
| 10.34** | 7.77** | 2 weeks | | |
| 0.18NS | 1 week | | | |
| 3 days | | | | |

【TRAP】

| | | | | |
|---|---|---|---|---|
| 6.36** | 5.20** | 0.06NS | 11.21** | 4 weeks |
| 34.44** | 31.67** | 9.63** | 3 weeks | |
| 7.65** | 6.37** | 2 weeks | | |
| 0.06NS | 1 week | | | |
| 3 days | | | | |

【CCAP】

| | | | | |
|---|---|---|---|---|
| 0 NS | 0 NS | 4.06** | 4.97** | 4 weeks |
| 4.97** | 4.97** | 0.05NS | 3 weeks | |
| 4.06** | 4.06** | 2 weeks | | |
| 0 NS | 1 week | | | |
| 3 days | | | | |

【CCTP】

| | | | | |
|---|---|---|---|---|
| 0 NS | 0 NS | 0.16NS | 11.69** | 4 weeks |
| 11.69** | 11.69** | 9.15** | 3 weeks | |
| 0.16NS | 0.16NS | 2 weeks | | |
| 0 NS | 1 week | | | |
| 3 days | | | | |

**:$p<0.01$
* :$p<0.05$

sample demonstrated nearly same histological features as those at 3 weeks, MGCs increased in size and number of nuclei (Figure 25, a).

    Enzyme-histochemically, positive rates of MGCs and their multiple comparison data in different materials are summarized in Tables 5 and 6. NSE staining showed a faintly diffuse positive reaction in the mononuclear cells but not in MGCs (Figure 25, b). A positive reaction
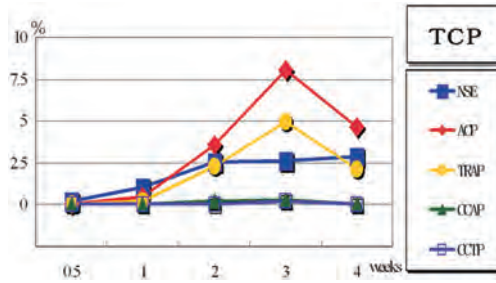
**Figure 23**   Time course of positive rate changes in
enzymatic activities after embedding
TCP.

was seen at 3 days and then it reached a peak at 4 weeks by gradually increasing (Figure 26). Mononuclear cells showed a diffuse-positive reaction of APC that was mostly located in the cytoplasms adjacent to BP granules. The number of positive cells was fewer than that of the HAP and TCP groups (Figure 25, c). The ACP-positive rate rose after 1 week in proportion to the time-course (Figure 26). TRAP reaction was faintly diffuse-cytoplasmic in a few mononuclear cells and MGCs (Figure 25, d) and its positive rate that was rising on the right and it was lower than that of ACP (Figure 26). CCAP reaction was infrequently found in a few mononuclear cells and MGCs. Diffuse positive features were restricted around vesicles that were phagocytozed in the cytoplasms (Figure 25, e). This positive rate was extremely lower than that of TRAP. CCAP reaction was only observed after 2 weeks and slightly increased at 4 weeks (Figure 26). Extremely weak CCTP reaction could be detected as a vesicular feature compatible with phagocytotic vacuoles of MGCs or mononuclear cells in only the case after 4 weeks (Figure 25, f). As shown in Figure 26, the positive rate remained almost at the baseline.

### 4)  MGCs induced via cholesterin (CHOL) embedding

Microscopically, embedded CHOL was observed as various-sized vacant spaces at 3 days. Numerous oval or spindle mononuclear cells infiltrated in the foci of aggregating vacuoles and surrounded them (Figure 27, a). However, the area with scattering CHOL spaces showed that mononuclear cells with oval eosinophilic cytoplasm were arranged in a doughnut shape around spaces. Infiltrated MGCs with a few nuclei were relatively small (Figure 27, b). At 1 week, most traces of CHOL became oval or ovoid spaces and MGCs, with 5 to 10 nuclei frequently showing cytoplasmic vacuoles that were considered as englobed cholesterin. These MGCs and mononuclear cells formed nodular granulation tissue (Figure 27, c). On the other hand, large CHOL spaces were surrounded by numerous MGCs and mononuclear cells arranged in doughnut shapes as seen at 3 days. In these nodules, some small clusters of mononuclear cells mimicked MGC with 2 to 5 nuclei because their cell borders were indistinct (Figure 27, d). At 2 weeks, MGCs increased in size, number, and number of nuclei and these showed doughnut-like or circular cytoplasm surrounding the embedded CHOL. As seen in other examples, nuclei of MGCs were flattened in the periphery but round in the center (Figure 27, e). After 3 weeks, MGCs increased in size and number of nuclei by the time-course, but they reduced their number. This artificial cholesterol granuloma appeared oval or ovoid nuclei in general but lacked cholesterol clefts like pine-needles that were frequently observed in inflammatory changes (Figure 27, f and Figure 28, a).

Enzyme-histochemically, positive rates of MGCs and their multiple comparison data in
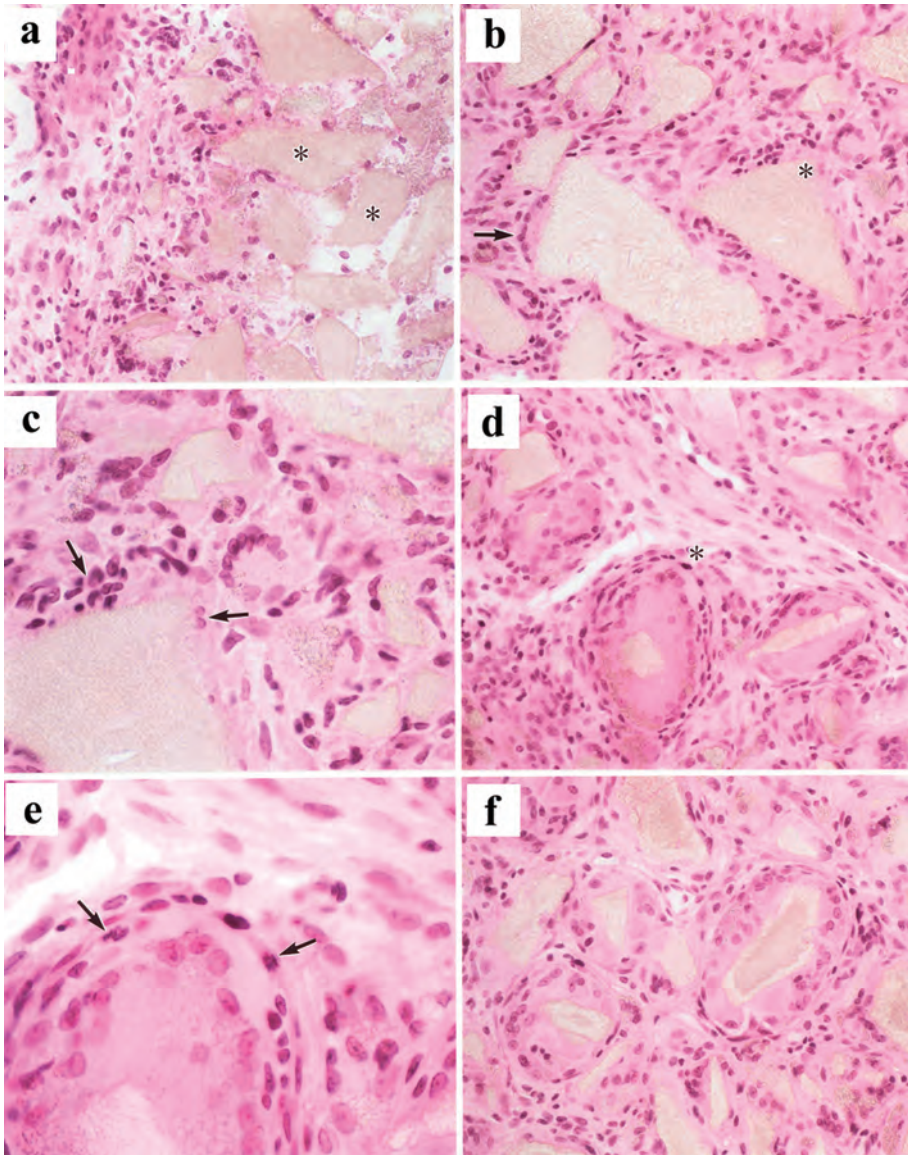
**Figure 24**　BP group

a: BP is found as the mass (asterisks) with mononuclear cell infiltration, 3 days after embedding.

b: Somewhat small MGCs (arrow) attached to granular masses, 1 week after embedding.

c: High power view of Figure b marked by an asterisk shows mononuclear cells with unclear cell border (arrow), 1 week after embedding.

d: Spindle mononuclear cells stack up around MGCs, 2 weeks after embedding.

e: High power view of the part marked by an asterisk in Figure d shows aggregated spindle cells with mitotic figures, 2 weeks after embedding.

f: The cell border of MGCs is considerably distinct, 3 weeks after embedding.
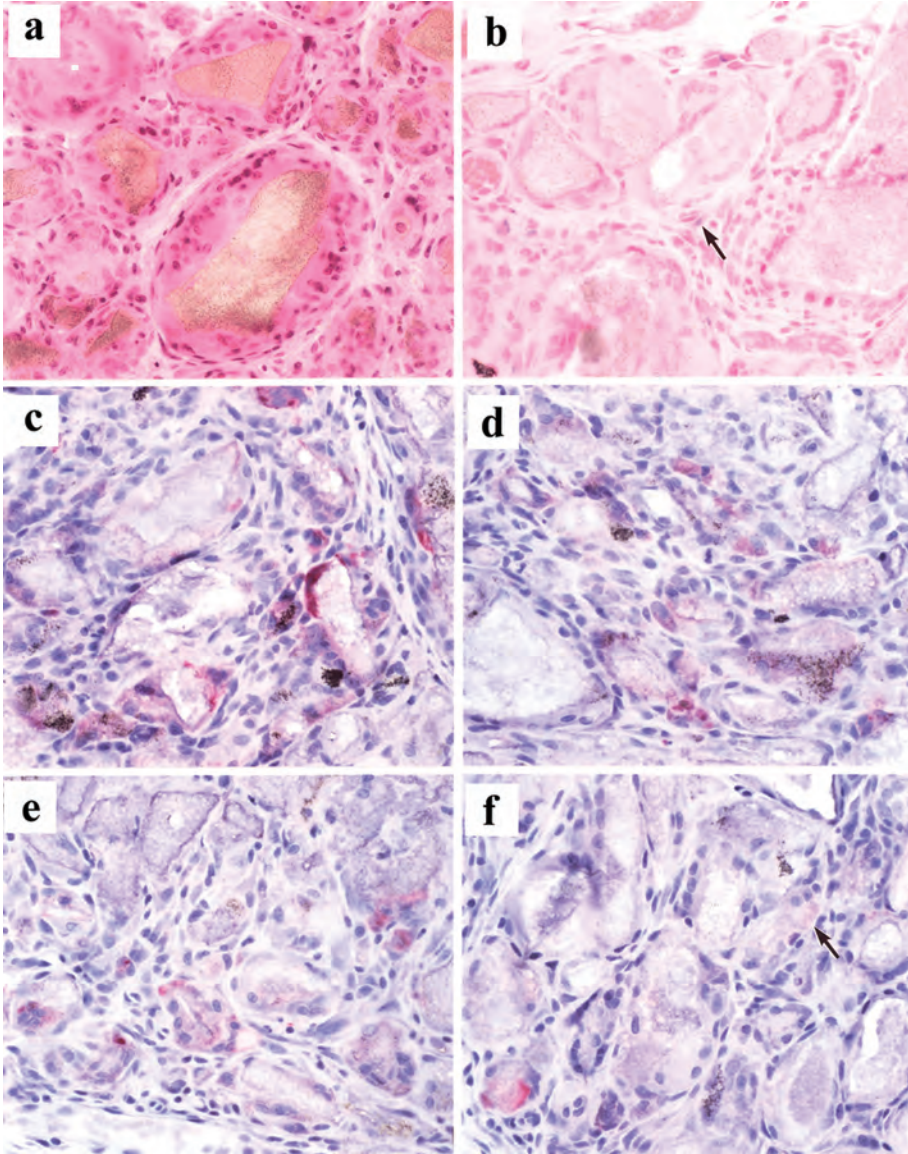
**Figure 25**  BP group

a:  The size of MGCs is same as that at 3 weeks but the number of nuclei increase, 4 weeks after embedding.

b:  NSE is negative in MGCs but in mononuclear cells (arrow), 4 weeks after embedding, NSE.

c:  Frequent ACP positive reactions are observed in cytoplasms of MGCS attached to BP, 4 weeks after embedding. ACP.

d:  Diffuse and weak TRAP positive reaction, 4 weeks after embedding. TRAP.

e:  Weak CCAP positive reaction in some mononuclear cells and MGCs, 4 weeks after embedding. CCAP.

f:  Note weak CCTP positive reaction (arrows) in the cytoplasms which show phagocytotic vacuoles, 4 weeks after embedding. CCTP.

**Table 5**   Positive rate of various enzyme activities in BP group

|      | 3 days | 1 week | 2 weeks | 3 weeks | 4 weeks |
|------|--------|--------|---------|---------|---------|
| NSE  | $0.34 \pm 0.020$ | $0.43 \pm 0.023$ | $0.61 \pm 0.019$ | $1.26 \pm 0.061$ | $2.02 \pm 0.047$ |
| ACP  | 0 | $0.43 \pm 0.065$ | $0.87 \pm 0.041$ | $1.37 \pm 0.706$ | $2.14 \pm 0.081$ |
| TRAP | 0 | $0.04 \pm 0.009$ | $0.32 \pm 0.012$ | $0.74 \pm 0.613$ | $1.63 \pm 0.094$ |
| CCAP | 0 | 0 | $0.05 \pm 0.024$ | $0.11 \pm 0.08$ | $0.25 \pm 0.056$ |
| CCTP | 0 | 0 | 0 | 0 | $0.01 \pm 0.004$ |

(Average ±Standard error; n=80, N=2000)

**Table 6**   Multiple comparisons using Scheffé's method of positive rates in BP group

【NSE】

| | | | | |
|---|---|---|---|---|
| 307.69** | 147.86** | 5.58** | 2.44** | 4 weeks |
| 255.29** | 112.29** | 0.64NS | 3 weeks | |
| 230.42** | 93.01** | 2 weeks | | |
| 28.96** | 1 week | | | |
| 3 days | | | | |

【ACP】

| | | | | |
|---|---|---|---|---|
| 18.81** | 15.28** | 1.26NS | 9.91** | 4 weeks |
| 56.00** | 49.78** | 18.21** | 3 weeks | |
| 10.34** | 7.77** | 2 weeks | | |
| 0.18NS | 1 week | | | |
| 3 days | | | | |

【TRAP】

| | | | | |
|---|---|---|---|---|
| 6.36** | 5.20** | 0.06NS | 11.21** | 4 weeks |
| 34.44** | 31.67** | 9.63** | 3 weeks | |
| 7.65** | 6.37** | 2 weeks | | |
| 0.06NS | 1 week | | | |
| 3 days | | | | |

【CCAP】

| | | | | |
|---|---|---|---|---|
| 0 NS | 0 NS | 4.06** | 4.97** | 4 weeks |
| 4.97** | 4.97** | 0.05NS | 3 weeks | |
| 4.06** | 4.06** | 2 weeks | | |
| 0 NS | 1 week | | | |
| 3 days | | | | |

【CCTP】

| | | | | |
|---|---|---|---|---|
| 0 NS | 0 NS | 0.16NS | 11.69** | 4 weeks |
| 11.69** | 11.69** | 9.15** | 3 weeks | |
| 0.16NS | 0.16NS | 2 weeks | | |
| 0 NS | 1 week | | | |
| 3 days | | | | |

**:p<0.01
* :p<0.05
NS:not significant

different materials were summarized in Tables 7 and 8. Diffuse and weak cytoplasmic reactions were seen in mononuclear cells around MGCs in NSE staining but MGCs and oval-swollen mononuclear cells seldom demonstrated positive reactions (Figure 28, b). The positive rate of this example showed a peak at 3 days and gradually declined for 4 weeks (Figure 29). Granular
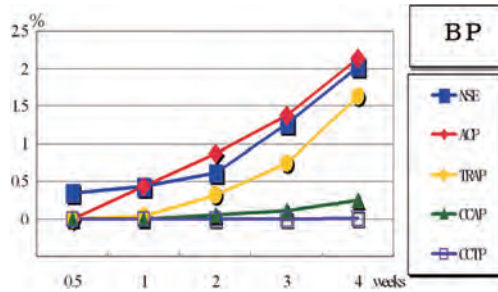
**Figure 26**  Time course of positive rate changes in
enzymatic activities after embedding
BP.

positive reaction for APC was found in mononuclear cells aggregating around CHOL spaces and some small MGCs. However, large MGCs were mostly negative (Figure 28, c). APC positive reactions were faintly observed at 3 days and showed a peak at 1 week, followed by gradual decreasing after 2 weeks (Figure 29). Reactivities of TRAP, CCAP and CCTAP were faintly demonstrated compared with that of NSE and APC. A weak positive reaction was mostly found in mononuclear cells around COHL spaces. A few small MGCs showing diffuse positive reactions were intermingled with negative MGCs (Figure 28, d). The line chart for TRAP positivity was nearly flat and a small increase was seen at 1 to 3 weeks (Figure 29). The level of CCAP reactivity was also extremely low, similar to TRAP. A positive reaction was only detected in mononuclear cells gathered around CHOL spaces (Figure 28, e). CCAP reaction was mostly negative and only showed extremely low positivity at 1 week and 2 weeks (Figure 29). There was no reaction of CCTP enzyme histochemistry in all periods (Figure 28, f and Figure 29). Moreover, no distinguishable feature was observed between enzyme-positive and negative cells in all groups.

## 5) Enzymatic characteristics of multinucleated giant cells (MGCs) under different conditions

Many previous studies reported on the enzymatic activity of MGCs induced by degradative or non-degradative materials. These data were not quantitative analyses but subjective ones such as "positive or negative", "many or few", "high or low", and so on [6, 24, 33, 54, 71]. Some investigations were assessed by the positive rate of mononuclear cells per all cells or per unit area [50, 59]. Our model was statistically analyzed after quantitative measurement (total 8, 000 points) using a color image analysis system.

As shown in Table 9, the analysis of variance of positive rates in each enzymatic reactivity revealed a statistical significant ($p < 0.01$) for all factors. Multiple comparisons using Scheffé's test indicated significant differences between values of all enzyme activities. ACP histochemistry showed the highest value, followed by TRAP, NSE, CCAP and CCTP (Table 10). The values of positive rates of the HAP group were the highest, followed by those of the TCP and BP groups. Although CHOL group showed the lowest values in all stainings, some values were statistically significant except values between TCP versus BP, and BP versus CHOL in CCAP staining, and BP versus CHOL in CCTP staining (Table 11). These results show the following: a) transition of positive rate of ACP is nearly similar to those of TRAP, CCAP and CCTP in every group; and b) positive rates of TRAP, CCAP and CCTP are lower than that of APC. MGCs generally appear after 5 to 7 days [37], which suggests that the intensity of tissue
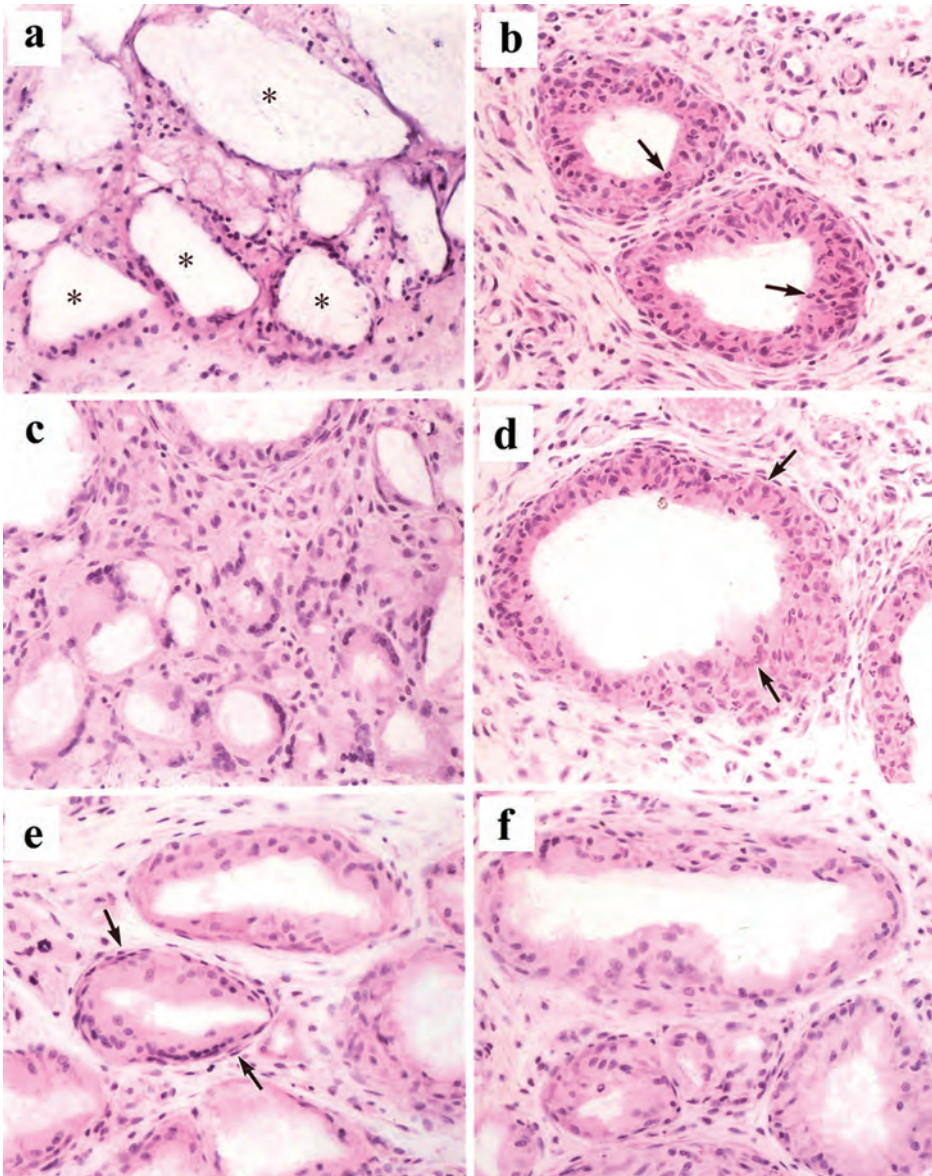
**Figure 27**  CHOL group

a:  Mononuclear cells surround vacant spaces of the trace of embedded CHOL (asterisks), 3 days after embedding.

b:  Mononuclear cells (arrows) are arranged in a doughnut shape with a few neutrophils, 1 week after embedding.

c:  Nodular proliferation of mono and multinucleated cells, 1 week after embedding.

d:  Small MGCs (arrows) appear in a doughnut shaped cell mass, 1 week after embedding.

e:  Most nuclei of MGCs in the periphery are flattened (arrows), 2 weeks after embedding.

f:  MGCs show an increase in size of their cytoplasms and number of nuclei, 3 weeks after embedding.
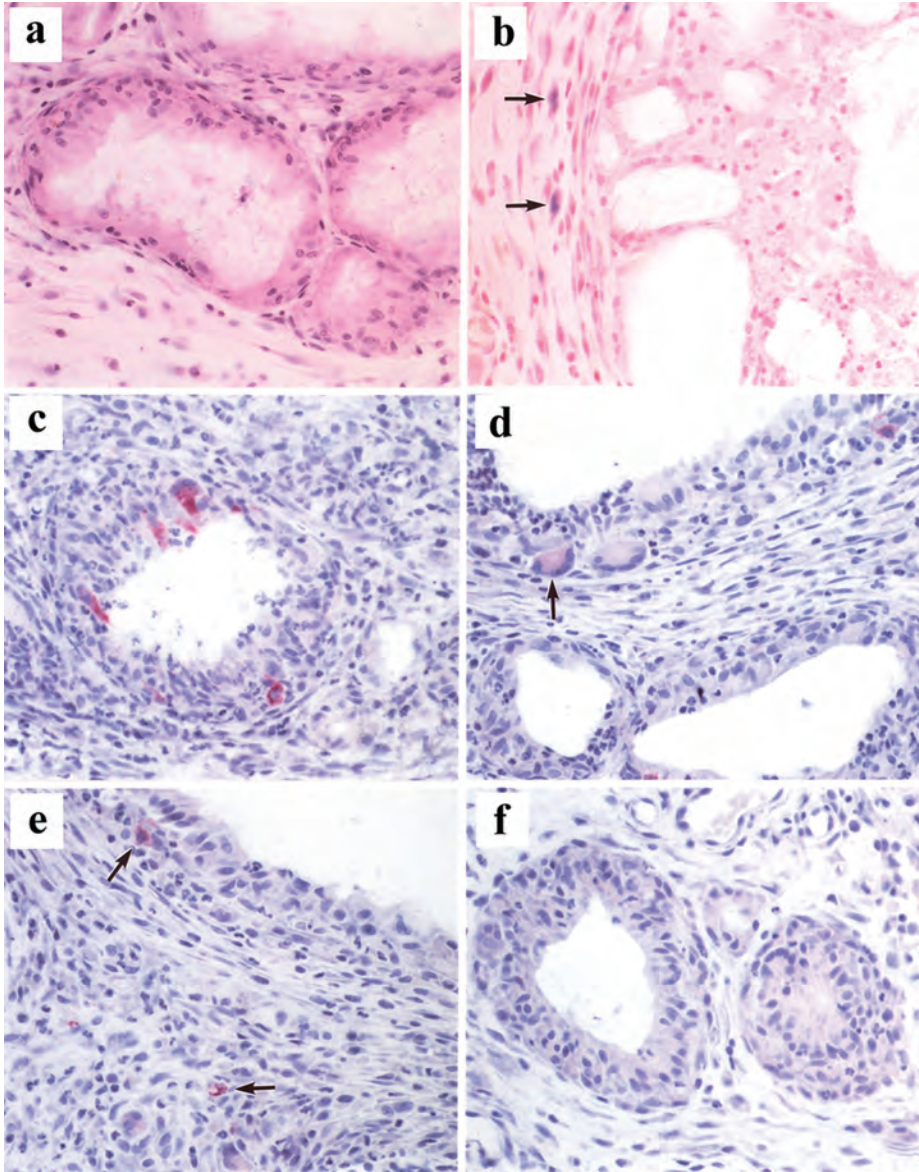
**Figure 28**    CHOL group

a:  MGCs show a more increase in size of their cytoplasms and number of nuclei similar to 3
    weeks cases, 4 weeks after embedding.

b:  NSE is only positive to spindle shaped mononuclear cells (arrows) in the periphery, 3 days
    after embedding, NSE.

c:  Some mononuclear cells and MGCs with a few nuclei show an ACP-positive reaction, 1 week
    after embedding. ACP.

d:  Note some MGCs are TRAP-weak positive (arrow) but others are negative, 1 week after
    embedding. TRAP.

e:  Granular positive reaction to a small number of mononuclear cells (arrows) is observed, 1
    week after embedding. CCAP.

f:  None of MGCs and mononuclear cells shows a positive reaction, 1 week after embedding.
    CCTP.

**Table 7**    Positive rate of various enzyme activities in CHOL group

|  | 3 days | 1 week | 2 weeks | 3 weeks | 4 weeks |
|---|---|---|---|---|---|
| NSE | 1.53 ± 0.020 | 1.39 ± 0.041 | 1.08 ± 0.041 | 1.08 ± 0.027 | 0.81 ± 0.028 |
| ACP | 0.01 ± 0.004 | 0.71 ± 0.024 | 0.24 ± 0.024 | 0.16 ± 0.021 | 0.02 ± 0.006 |
| TRAP | 0 | 0.08 ± 0.012 | 0.05 ± 0.012 | 0.03 ± 0.005 | 0 |
| CCAP | 0 | 0.02 ± 0.001 | 0.01 ± 0.001 | 0 | 0 |
| CCTP | 0 | 0 | 0 | 0 | 0 |

(Average ±Standard error ;    n=80, N=2000)

**Table 8**    Multiple comparisons using Scheffé's method of positive rates in TCP group

【NSE】

| | | | | |
|---|---|---|---|---|
| 44.05** | 28.41** | 7.99** | 6.18** | 4 weeks |
| 17.24** | 8.09** | 0.12NS | 3 weeks | |
| 15.53** | 6.27** | 2 weeks | | |
| 1.71NS | 1 week | | | |
| 3 days | | | | |

【ACP】

| | | | | |
|---|---|---|---|---|
| 0.01NS | 44.21** | 4.36** | 1.76NS | 4 weeks |
| 2.06NS | 28.32** | 0.58NS | 3 weeks | |
| 4.81** | 20.80** | 2 weeks | | |
| 45.63** | 1 week | | | |
| 3 days | | | | |

【TRAP】

| | | | | |
|---|---|---|---|---|
| 0 NS | 9.84** | 3.16** | 0.89NS | 4 weeks |
| 0.89NS | 4.81** | 0.69NS | 3 weeks | |
| 3.16* | 1.85NS | 2 weeks | | |
| 9.84** | 1 week | | | |
| 3 days | | | | |

【CCAP】

| | | | | |
|---|---|---|---|---|
| 0 NS | 2.82* | 0.27NS | 0 NS | 4 weeks |
| 0 NS | 2.82* | 0.27NS | 3 weeks | |
| 0.27NS | 1.35NS | 2 weeks | | |
| 2.82* | 1 week | | | |
| 3 days | | | | |

【CCTP】

| | | | | |
|---|---|---|---|---|
| 0 NS | 0 NS | 0 NS | 0 NS | 4 weeks |
| 0 NS | 0 NS | 0 NS | 3 weeks | |
| 0 NS | 0 NS | 2 weeks | | |
| 0 NS | 1 week | | | |
| 3 days | | | | |

**:$p<0.01$
* :$p<0.05$

reaction to embedded materials might reach its peak at about 1 week. Three days after embedding, only limited MGCs appeared in the foci which were small in size and had a few nuclei. Then MGC increased in size and number after 3 weeks. Foreign body reaction or granuloma is one type of chronic inflammation that is caused by cell-mediated immunity. In the
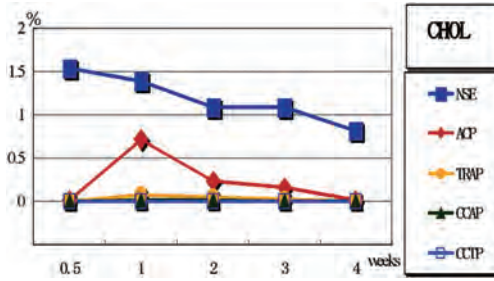
**Figure 29**   Time course of positive rate changes in enzymatic activities after embedding CHOL.

acute phase, infiltration of macrophages is maximally activated at 3 days. MGCs mostly appear for 2 weeks in both intraosseous and extraosseous tissues. Mariano and Specter [43] suspected that the life span of MGCs was 6 days after formation based on a quantitative analysis. This hypothesis seems to be appropriate because peaks of enzyme activities are at 2 or 3 weeks after embedding of non-degradative materials. However, in cases of degradative materials, the formation of MGCs might be continuing until the embedded materials are completely absorbed. This is why enzyme activity gradually rises over time in the case of sterilized bovine bone particles.

The environments of embedded material are also important for MGC formation. Implantation of artificial bone within intraosseous or parosteal tissues are able to induce osteoclast-like MGCs resorbing embedded materials [33, 52]. In this condition, it is impossible to distinguish whether MGCs were originally located or MGCs experimentally induced. Moreover, there is a possibility that MGCs are not induced by embedded ceramics but by originally existing factors. Naturally, osteoclasts cannot be derived in soft tissues, such as subcutaneous tissue, so that MGCs induced in this model are not osteoclasts. Activities of

**Table 9**   Analysis of variance in positive rate of enzyme activities

| factor | S | d.f. | V | Fo |
|---|---|---|---|---|
| A:material | 11147.605 | 3 | 3715.869 | 1161.935** |
| B:enzyme | 11897.396 | 4 | 2974.349 | 930.065** |
| C:period | 5824.215 | 4 | 1456.054 | 455.301** |
| A×B | 13823.883 | 12 | 1151.990 | 360.222** |
| A×C | 6776.717 | 12 | 564.726 | 176.587** |
| B×C | 5714.436 | 16 | 357.152 | 111.679** |
| error | 25417.775 | 7948 | 3.198 | |
| total | 69454.422 | 7999 | | |

**: $P < 0.01$

**Table 10**   Multiple comparisons using Scheffé's method of positive rates by ezyme activities

| | | | | |
|---|---|---|---|---|
| 141.09** | 123.63** | 155.53** | 441.84** | NSE |
| 1082.28** | 1032.90** | 73.08** | ACP | |
| 592.89** | 556.49** | TRAP | | |
| 0.58NS | CCAP | | | |
| CCTP | | | | |

**: $p < 0.01$
*: $p < 0.05$

**Table 11** Multiple comparisons using Scheffé's method of positive rates of enzyme activities by embeded meterials

【NSE】

| | | | |
|---|---|---|---|
| 283.608** | 472.580** | 11.979** | HAP |
| 179.014** | 334.080** | TCP | |
| 23.993** | BP | | |
| CHOL | | | |

【ACP】

| | | | |
|---|---|---|---|
| 625.156** | 522.269** | 255.400** | HAP |
| 81.395** | 47.244** | TCP | |
| 4.622** | BP | | |
| CHOL | | | |

【TRAP】

| | | | |
|---|---|---|---|
| 633.313** | 513.841** | 256.400** | HAP |
| 83.930** | 44.405** | TCP | |
| 6.238** | BP | | |
| CHOL | | | |

【CCAP】

| | | | |
|---|---|---|---|
| 23.842** | 12.937** | 10.907** | HAP |
| 2.497* | 0.087NS | TCP | |
| 1.654N S | BP | | |
| CHOL | | | |

【CCTP】

| | | | |
|---|---|---|---|
| 30.973** | 29.985** | 10.626** | HAP |
| 5.316** | 4.912** | TCP | |
| 0.008NS | BP | | |
| CHOL | | | |

**: $p < 0.01$
*: $p < 0.05$

TRAP, CCAP and CCTP are those of ACP after inhibition by tartrate acid, cyanuric chloride and both, respectively. CCAP and CCTP are able to identify a more restricted population in the osteoclastic lineage than that detected by TRAP staining [50]. In this sense, MGC induced by HAP or TCP could be considered to belong to a family of osteoclasts.

Most MGCs show enzymatic activity similar to that of osteoclasts/odontoclasts: NSE negative, ACP or TRAP positive [47, 71]. NSE positive rates of mononuclear cells gradually increased in the HAP, TCP and BP group but decreased in the CHOL group. In other words, the supply of NSE positive macrophages lasts for a relatively longer time in HAP, TCP and BP than in CHOL. Macrophages change their NSE positive nature to NSE negative after multi-nucleation. Positive rates of ACP and TRAP are extremely high in HAP, TCP and BP so that the evaluation of TRAP activity is useful for the identification of osteoclasts or osteoclast-like cells (Figure 30). Generally, TRAP has been used as a specific marker of osteoclast [5, 47, 50, 51, 71] but it can be detected in alveolar macrophages [50, 59], splenic macrophage, proximal uriniferous tubules and some hepatocytes, osteoblasts and osteocytes (12). Some foreign body giant cells also are TRAP positive not only in artificial bone graft (6) but also cholesterol granulomas. This result show that TRAP is not a complete marker of osteoclasts. CCAP and
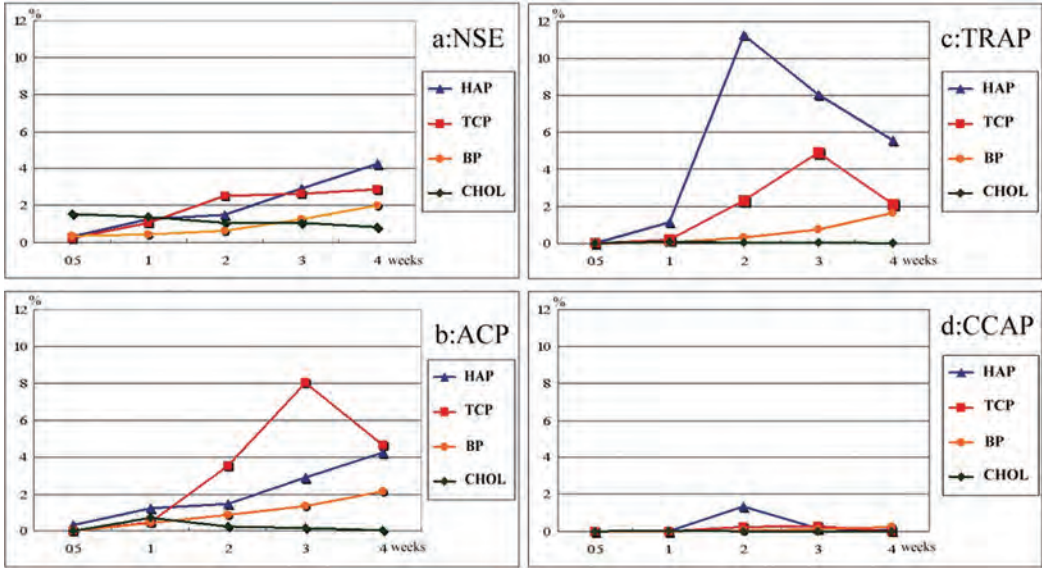
**Figure 30** Time-course of enzyme activities; a: NSE, b: ACP, c: TRA and d: CCAP show different enzyme activities and chart lines in embedding different materials. These chart lines seem to depend on the properties of embedded materials. Y-axis scale (positive rate) of all graphs is aligned. Positive rates of CCAP and TRAP in CHOL group are below 1%, so these lines are on the baseline.

CCTP are more specific as markers for osteoclasts than is TRAP (50), which is confirmed by multiple comparison tests of our data. After 3 days, MGCs were mostly TRAP negative but turned TRAP positive after 1 week. Even in the CHOL group, CCAP positive cells were faintly present after 1 to 2 weeks (Figure 30). In any foreign body reactions, MGCs slightly demonstrate tartrate or cyanuric chloride resistant ACP activities at an early stage but cannot maintain these enzymatic activities. MGCs seem to stop enzymatic activities because these do not require the phagocytotic function in cholesterol granuloma. On the other hand, in deproteinized and sterilized bone particles (BP), MGCs continue to maintain TRAP-/CCAP activity for englobing hard tissue. These enzymatic activities seem to represent the functional status of multinucleated giant cells.

### 6) Formation and nature of multinucleated giant cells (MGCs)

Many investigators have accepted that foreign body giant cells and osteoclasts are formed through cell fusion of monocytes/macrophages [13, 18, 24, 25, 32, 43]. Infiltrated mononuclear cells are NSE-positive and partially APC-positive, which is an enzymatic characteristic of macrophages. NSE-positive spindle cells frequently pile up around embedded materials, and they closely contact each other and finally lose cell borders. Similar to ultrastructural features of part 1, macrophages change their round cytoplasm to a flat one at first, followed by elongation and contact of cytoplasmic processes like pseudopodia, and finally membrane fusion. As described above, CD36 participates in cell fusion and works at the cell fusion site. In addition to CD36, recognition of phosphatidylserine is also required for macrophage polykaryon formation [31]. On cell fusion, old macrophages seem to recognize immature ones [43]. In the early stage (at 1 or 2 weeks) of our subcutaneous model, MGCs with a few nuclei were relatively small, while MGCs were large and they decreased in number in the late stage (at 3 and 4 weeks). This suggests that large MGCs were made by fusion of small MGCs. Osteoclast formation requires

the presence of mononuclear marrow cells having a mitotic ability *in vitro* [17]. Many mitoses of mononuclear cells around embedded material may satisfy a factor of giant cell formation. In addition, mitotic features were rarely observed in giant cells of the HAP group at 2 weeks when giant cell formation was most active. This provides the possibility of giant cell formation by mitosis without division. Taking together the features of both periodontal tissue and soft tissue, mitosis is an important phenomenon for multinucleated giant cell formation in various tissues.

Non-degradative or degradative properties of embedded materials come out as different histological appearances in this experiment. Although their morphological features seem to be somewhat different from those of clinical cases such as Figure 18, these differences might to be caused by components of mixtures or by observation periods. On the other hand, CHOL is an organic substance that is frequently found in oral lesions such as radicular cysts or radicular granulomas [15, 64]. As shown in Figure 31, a characteristic feature of cholesterol granuloma or foreign body granuloma is scattered vacant spaces similar to pine needles, while traces of CHOL were oval or ovoid vacant spaces in the current experiment. However, in all examples, non-organic or organic material can induce numerous spindle-shaped macrophages and MGCs with variable features. There are intimate relationships between the size of embedded materials and their processing manner. Particles measuring 5 to 10 $\mu$m, 6 to 15 $\mu$m 10 to 15 $\mu$m or even over 7 $\mu$m, can be processed by macrophages and MGCs [65]. In this model, all embedded particles were prepared to be under 20 $\mu$m, so that MGCs might efficiently induced.

Prior to phagocytosis, macrophages seem to recognize the size or nature of a foreign body. If a foreign body was too large to phagocytose for a single macrophage, macrophages might process the foreign body after alteration to a multinucleated giant cell. Namely, it could be that macrophages alter the phagocytic method according to the kind of foreign body. In the model of reaction to various kinds of foreign bodies such as HAP, TCP, BP and CHOL, pathological features are somewhat different. The morphological characteristic of MGC is roughly divided into two types; oval and irregular. The former shows small cytoplasm including fine granules, while the later mostly attaches to large embedded granules or aggregates of materials. As with macrophages, morphological characteristics of MGCs might depend upon the size of the foreign body. In case the material is easily englobed, MGC shows a small and oval shape. However, MGC changes its cytoplasm and simultaneously surrounds an object that is difficult to englobe
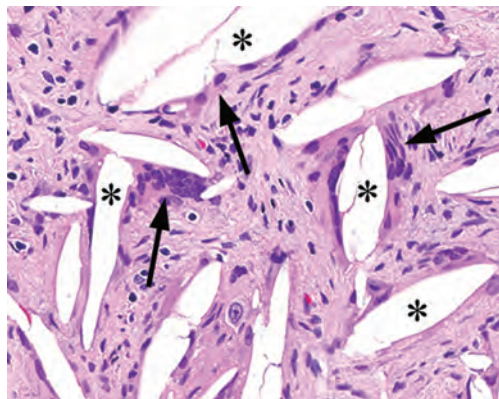


**Figure 31**  Inflammatory MGCs induced by cholesterol: Some multinucleated giant cells (arrows) appear around cholesterol clefts (asterisks).

[65]. Therefore, the outline of MGC depends upon the form of the material [20, 41, 48].

Ultrastructural investigations previously reported to show that MGC occasionally has a ruffled border and clear zone [24, 25, 32, 39] but not in most cases. MGC arising in the bone tissue with HAP implantation frequently demonstrated a ruffled border and clear zone [33, 52]. Contrarily, not all giant cells found in dentin resorption (shown in Figure 11) have these structures.

Ruffled border-like structure is found in the case of HAP baked at 200°C but not in cases treated at 1,250°C, which means that the physicochemical nature is one important factor for osteoclast differentiation [66]. The microenvironment, which could be affected by the property of artificial bone, is an important factor of osteoclast differentiation. Different materials embedded within tissues may affect the microenvironment *in vivo*. In fact, hyponatremia affects sodium signaling mechanisms in osteoclasts and leads to a resorptive osteoporosis [10]. Macrophages or MGCs are capable of altering their shape and function according to the properties of their targets.

## References

[1]   Abe E, Ishimi Y, Takahashi N, Akatsu T, Ozawa H, Yamana H, Yoshiki S and Suda T (1988) A differentiation-inducing factor produced by the osteoblastic cell line MC3T3-E1 stimulates bone resorption by promoting osteoclast formation. J Bone Miner Res. 3 (6): 635-645.

[2]   Abe E, Miyaura C, Tanaka H, ShiinaY, Kuribayashi T, Suda S, Nishii Y, Deluca HF and Suda T (1983) 1α, 25-dihydroxy vitamin D3 promotes fusion of mouse alveolar macrophages both by a direct mechanism and by aspleen cell-mediated indirect mechanism. Proc Natl Acad Sci USA 80: 5583-5587.

[3]   Adams DO (1974) The structure of mononuclear phagocytes differentiating in vivo. I. Sequential fine and histologic study of the effect of Bacillus Calmette-uerin (BCG). Am J Pathol 76: 18-48.

[4]   Anderson JM, Rodriguez A and Chang DT (2008) Foreign body reaction to biomaterials. Semin Immunol 20(2): 86-100.

[5]   Akisaka T, Subita GP, Kawaguchi H and Shigenaga Y (1989) Different tartrate sensitivity and PH optimum for two isoenzymes of acid phosphatase in osteoclasts. An electronmicroscopic enzyme-cytochemical study. Cell Res 255: 69-76.

[6]   Antoh M, Kawakami T, Hasegawa H and Eda S. Tartrate-resistant acid phosphatase activity in multinucleated giant cells appearing in cholesterin granulomas induced experimentally in rats. Med Sci Res 20: 298-294.

[7]   Athanasou NA and Quinn J (1990) Immunophenotypic differences between osteoclasts and macrophage polykaryons: immunohistological distinction and implications for osteoclast ontogeny and function. J Clin Pathol 43 (12): 997-1003.

[8]   Athanasou NA, Wells CA, Quinn J, Ferguson DP, Heryet A and McGee JO (1989) The origin and nature of stromal osteoclast-like multinucleated giant cells in breast carcinoma: implications for tumour osteolysis and macrophage biology. Br J Cancer 59 (4): 491-498.

[9]   Baron R, Neff L, Van PT, Nefussi J and Vignery A (1986) Kinetic cytochemical identification of osteoclast precursors and their differentiation into multinucleated osteoclasts. J Pathol 122: 363-378.

[10]  Barsony J, Sugimura Y and Verbalis JG (2011) Osteoclast response to low extracellular sodium and the mechanism of hyponatremia-induced bone loss. J Biol Chem 286(12): 10864-75. Epub 2010 Dec 6. .

[11]  Bianco P, Costantini M, Dearden LC and Bonucci E (1987) Expression of tartrate-resistant acid phosphatase in bone marrow macrophages. Basic Appl Histochem 31: 433-440.

[12]  Bianco P, Ballanti P and Bonucci E (1988) Tartrate-resistant acid phosphatase activity in rat osteoblasts and osteocytes. Calcif Tiss Int 43: 167-171.

[13]  Bird MC, Garside D and Jones HB (1992) Multinucleated giant cells in primary cultures derived from canine bone marrow evidence for formation of putative osteoclasts. Cell Tiss Res 268: 17-30.

[14]  Black MM and Epstain WL (1974) Formation of mononucleate giant cells in organized epitheloid cell granulomas. Am J Pathol 74: 263-274.

[15]  Browne RM (1971) The origin of cholesterol in odontogenic cysts in man. Arch Oral Biol 16: 107-113.

[16]  Brudvik P and Rygh PB (1993) The initial phase of orthodontic root resorption incident to local compression of the periodontal ligament. Eur J Orthod 15(4): 249-263.

[17]   Burger EH, Van Der Meer JW, Van De Gevel JS, Gribnau JC, Thesingh CW and Van Furth R (1982) In vitro formation of osteoclasts from long-term cultures of bone marrow mononuclear phagocytes. J Exp Med 156: 1604-1614.

[18]   Chambers TJ (1978) Multinucleated giant cell. J Pathol 126: 125-148.

[19]   Donath K, Laass M and Günzl HJ (1992) The histopathology of different foreign-body reactions in oral soft tissue and bone tissue. Virch Arch A Pathol Anat Histopathol 420 (2): 131-137.

[20]   Drobeck HP, Rothstein SS, Gumaer KI, Sherer AD and Slighter RG (1984) Histologic observation of soft tissue responses to implanted, multifaceted particles and discs of hydroxyapatite. J Oral Maxillofac Surg 42: 143-149.

[21]   Evan EJ (1991) Toxicity of hydroxyapatite in vitro: the effect of particle size. Biomaterials 12: 574-576.

[22]   Freilich LS (1971) Ultrastructure and acid phosphatase cytochemistry of odontoclasts: effects of parathyroid extract. J Dent Res 50: 1046-1055.

[23]   Ganeles J, Listgarten MA and Evian CI (1986) Ultrastrucuture of durapatite-periodontal tissue interface in human intrabony defects. J Periodontol 57: 133-140.

[24]   Glowacki J and Cox KA (1986) Osteoclastic features of cells that resorb bone implants in rats. Calcif Tiss Int 39: 97-103.

[25]   Glowacki J, Jasty M and Goldring S (1986) Comparison of multinucleated cells elicited in rats by particulate bone, polyethylene or polymethylmethacrylate. J Bone Mineral Res 1: 327-331.

[26]   Goldberg RD, Michelassi F and Montag AG (1991) Osteoclast-like giant cell tumor of the pancreas: immunophenotypic similarity to giant cell tumor of bone. Hum Pathol 22: 618-622.

[27]   Graves D (2008) Cytokines that promote periodontal tissue destruction. J Periodontol 79: 1585-1591.

[28]   Harokopakis-Hajishengallis E (2007) Physiologic root resorption in primary teeth: molecular and histological events. J Oral Sci 49: 1-12.

[29]   Hattersley G, Owens J, Flanagan AM and Chambers TJ (1991) Macrophage colony stimulating factor (M-CSF) is essential for osteoclast formation in vitro. Biochem Biophys Res Commun 177: 526-531.

[30]   Haythorn SR (1929) Multinucleated giant cells. Arch Pathol 7: 651-713.

[31]   Helming L, Winter J and Gordon S (2009) The scavenger receptor CD36 plays a role in cytokine-induced macrophage fusion. J Cell Sci 122: 453-459.

[32]   Holtrop ME, Cox KA and Glowacki J (1982) Cells of the mononuclear phagocytic system resorb implanted bone matrix: a histologic and ultrastructuralstudy. Calcif Tiss Int 34: 488-494.

[33]   Kawaguchi H, Ogawa T, Shirakawa M, Okamoto H and Akisaka, T (1992) Ultrastructural and ultracytochemical characteristics of multinucleated cells after hydroxyapatite implantation into rat periodontal tissue. J Periodont Res 27: 48-54.

[34]   Kawakami T, Nakamura C, Hasegawa H and Eda S (1987) Fate of[14]C-labelled dimethylpoly-siloxane (silicone oil) in a root canal filling material embedded in rat subcutaneous tissues. Dent Mater 3: 256-260.

[35]   Kawakami T, Nakamura C, Hasegawa H and Eda S (1987) Fate of ^{14}C-labelled calcium hydroxide in a root canal filling paste embedded in rat subcutaneous issues. J Endod 13: 220-223.

[36]   Kawakami T, Nakamura C, Hasegawa H, Akahane S and Eda S (1987) Ultrastructural study of initial calcification in the rat subcutaneous tissues elicited by root canal filling material. Oral Surg 63: 360-365.

[37]   Klein CPAT, Blieck-Hogervorst JMA, Wolke JGC and do Groot K (1990) Studies of the solubility of different calcium phosphate ceramic particles in vitoro. Biomaterials 11: 509-517.

[38]   Klein CPAT, Driessen AA, de Greet K and van den Hooff A (1983) Biodegradation behavior of various calcium phosphate materials in bone tissue. J Biomed Mater Res 17: 769-784.

[39]   Krukowski M and Kahn AJ (1982) Inductive specificity of mineralized bone matrix in ectopic osteoclast differentiation. Calcif Tiss Int 34: 474-479.

[40]   Lee MS, Kim HS, Yeon JT, Choi SW, Chun CH, Kwak HB and Oh J (2009) GM-CSF regulates fusion of mononuclear osteoclasts into bone-resorbing osteoclasts by activating the Ras/ERK pathway. Immuno. 183: 3390-3399.

[41]   Lee YM, Fujikado N, Manaka H, Yasuda H and Iwakura Y (2010) IL-1 plays an important role in the bone metabolism under physiological conditions. Int Immunol 22: 805-816.

[42]   Lehtinen R, Kuusilehto A and Nikkanen U (1990) Bone response to hydroxyapatite particles of different shapes in rabbit tibia. J Oral Maxillofac Surg 48: 1075-1078.

[43]   Mariano M and Spector WG (1974) The formation and properties of macrophage polykaryons (inflammatory giant cell). J Patho1 113: 1-18.

[44]   Marks SC Jr, Donald DR and Wise GE (1983) The cytology of the dental follicle and adjacent alveolar bone during tooth eruption in the dog. Am J Anat 168: 277-279.

[45]   Marks SC Jr and Grolman M (1987) Tartrate-resistant acid phosphatase in mononuclear and multinuclear cells during the bone resorption of tooth eruption. J Histochem Cytochem 35: 1227-1230.

[46]   Mii Y, Miyauchi Y, Morishita T, Miura S, Honoki K, Aoki M and Tamai S (1991) Osteoclast origin of giant cells in

giant cell tumors of bone: Ultrastructural and cytochemical study of six cases. Ultrastruct Pathol 5: 623-629.

[47]   Minkin C (1982) Bone acid phosphatase: Tartrate-resistant acid phosphatase as marker of osteoclast function. Calcif Tissue Int 34: 285-290.

[48]   Misiek DJ, Kent JN and Carr RF (1984) Soft tissue responses to hydroxyapatite particles of different shapes. J Oral Maxillofac Surg 42: 150-160.

[49]   Nagahara K, Isogai M, Shibata K and Meenaghan AM (1992) Osteogenesis of hydroxyapatite and tricalcium phosphate used as a bone substitute. Int J Maxillofac Implant 7: 72-79.

[50]   Nakamura Y, Yamaguchi A, Ikeda T and Yoshiki S (1991) Acid phosphatase activity is detected preferentially in the osteoclastic lineage by pre-treatment with cyanuric chloride. J Histochem Cytochem 39: 1415-1420.

[51]   Nijweide PJ, Burger EH and Feyen JHM (1986) Proliferation, differentiation and hormonal regulation. Physiol Rev 66: 855-856.

[52]   Ogilvie A., Frank RM, Benque EP, Gineste M, Heughebaert M and Hemmerle J (1987) The biocompatibility of hydroxy-apatite implanted in the human periodontium. J Periodont Res 22: 270-283.

[53]   Owens J and Chambers TJ (1993) Macrophage colony-stimulating factor (M-CSF) induces migration in osteoclasts in vitro. Biochem Biophys Res Commun 195(3): 1401-1407.

[54]   Pettls GY, Kaban LB and G1owacki J (1990) Tissue response to composite ceramic hydroxyapatite/demineralized bone implants. J OralMaxillofac Surg 48: 1068-1074.

[55]   Popova A, Kzhyshkowska J, Nurgazieva D, Goerdt S and Gratchev A (2011) Pro- and anti-inflammatory control of M-CSF-mediated macrophage differentiation. Immunobiology 216 (1, 2): 164-712.

[56]   Quinn JM, Athanasou NA and McGee JO (1991) Extracellular matrix receptor and platelet antigens on osteoclasts and foreign body giant cells. Histochemistry 96(2): 169-176.

[57]   Quinn JM, Horwood NJ, Elliott J, Gillespie MT and Martin TJ (2000) Fibroblastic stromal cells express receptor activator of NF-kappa B ligand and support osteoclast differentiation. J Bone Miner Res 15(8): 1459-1466.

[58]   Quinn JM, Neale S, Fujikawa Y, McGee JO and Athanasou NA (1998) Human osteoclast formation from blood monocytes, peritoneal macrophages, and bone marrow cells. Calcif Tissue Int 62(6): 527-531.

[59]   Radzun HJ, Kreipe H and Parwaresch MR (1983) Tartrate-resistant acid phosphatase as a differentiation marker for the human mononuclear phagocyte system. Hematol Oncol 1: 321-327.

[60]   Sabokbar A, Pandey R, Díaz J, Quinn JM, Murray DW and Athanasou NA (2001) Hydroxyapatite particles are capable of inducing osteoclast formation. J Mater Sci Mater Med 12 (8): 659-664.

[61]   Sasaki T and Matsuda U (1993) Imunocytochemical localization of cathepsin B and G in odontoclasts of human deciduous teeth. J Dent Res 71: 1881-1884.

[62]   Sasaki T, Shimizu T, Watanabe C and Hiyoshi Y (1990) Cellular roles in physiological root resorption of deciduous teeth in the cat. J Dent Res 69: 67-74.

[63]   Sasaki T, Watanabe C, Shimizu T, Debari K and Segawa K (1990) Possible role of cementoblasts in the resorbant organ of human deciduous teeth during root resorption. J Periodont Res 25: 143-151.

[64]   Shear M (1988) Cholesterol in dental cysts. Oral Surg 16: 1465-1473.

[65]   Shimizu S (1988) Subcutaneous tissue responses in rats to injection of fine particles of synthetic hydroxyapatite ceramic. Biomedical Res 9: 95-111.

[66]   Takeshita N, Akagi T, Yamasaki M, Ozeki T, Nojima T, Hiramatsu Y and Nagai N (1992) Osteoclastic features of multinucleated giant cells responding to synthetic hydroxy-apatite implanted in rat jaw bone. J Electron Microsc 41: 141-146.

[67]   Tanabe N, Maeno M, Suzuki N, Fujisaki K, Tanaka H, Ogiso B and Ito K (2005) IL-1 alpha stimulates the formation of osteoclast-like cells by increasing M-CSF and PGE2 production and decreasing OPG production by osteoblasts. Life Sci 77 (6): 615-626.

[68]   Ten Cate AR and Anderson RD (1986) An ultrastructural study of tooth resorption in the kitten. J Dent Res 65: 1087-1097.

[69]   Udagawa N, Takahashi N, Akatsu T, Tanaka H, Sasaki T, Nishihara T, Koga T, Martin TJ, and Suda T (1990) Origin of osteoclast: mature monocytes and macrophages are capable of differentiating into osteoclasts under a suitable microenvironment prepared by bone marrow-derived stromal cells. Proc Natl Acad Sci USA. 87: 7260-7264.

[70]   Udagawa N, Takahashi N, AkatsuT, Tanaka H, SasakiT, Yamaguchi A, Kodama H, Martin TJ and Suda T (1989) The bone marrow-derived stromal cell lines MC3T3-G2/PA6 and ST2 support osteoclast-like cell differentiation in co-cultures with mouse spleen cells. Endocrinology 125: 1805-1813.

[71]   Van de Wijngaert FP and Burger EH (1986) Demonstration of tartrate-resistant acid phosphatase in undecalcified, glycolmethacrylate-embedded mouse bone: a possible marker for (pre)osteoclast identification. J Histochem Cytochem 34: 1317-1323.

[72]   Wiktor Jedrzejczak W, Urbanowska E, Aukerman SL, Pollard JW, Stanley ER, Ralph P, Ansari AA, Sell KW and Szperl M (1991) Correction by CSF-1 of defects in the osteopetrotic op/op mouse suggests local developmental and humoral reqirements for this growth factor. Exp Hematol 19: 1049-1054.

[73]   Wiktor-Jedrzejczak W, Bartocci A, Ferrante AW Jr, Ahmed-Ansari A, Sell KW, Pollard JW and Stanley ER (1990) Total absence of colony-stimulating factor 1 in the macrophage-deficient osteopetrotic (op/op) mouse. Proc Natl Acad Sci USA 87 (12): 4828-4832.

[74]   Wise GE (2009) Cellular and molecular basis of tooth eruption. Orthod Craniofac Res 12 (2): 67-73.

[75]   Wise GE, Marks SC Jr and Cahill DR (1985) Ultrastructural features of the dental follicle associated with formation of the tooth eruption pathway in the dog. J Oral Pathol 14: 15-26.

[76]   Wise GE and Yao S (2003) Expression of vascular endothelial growth factor in the dental follicle. Crit Rev Eukaryot Gene Expr 13 (2-4): 173-180.

[77]   Zhu H, Jiang XX, Guo ZK, Li H, Su YF, Yao HY, Wang XY, Li XS, Wu Y, Liu YL, Zhang Y and Mao N (2009) Tumor necrosis factor-alpha alters the modulatory effects of mesenchymal stem cells on osteoclast formation and function. Stem Cells Dev 18 (10): 1473-184.

Address for Correspondence: Professor Hiromasa Hasegawa, Department of Oral Pathology, Matsumoto Dental University School of Dentistry, Shiojiri, 399-0781 Japan
    Phone：＋81-263-51-2092, Fax：＋81-263-51-2093, E-mail：hasegawa@po.mdu.ac.jp